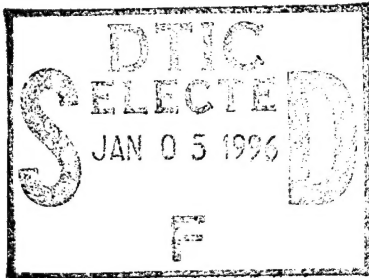Final Technical Report to
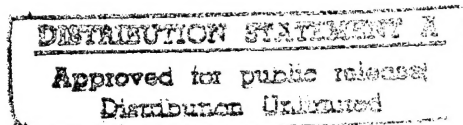The Office of Naval Research
and
SDIO/BMDO
for the Project:

"Theoretical and Experimental Studies of a
Novel Accelerating Structure"
N00014-91-J-1941

R. M. Gilgenbach and Y. Y. Lau
Intense Energy Beam Interaction Laboratory
Nuclear Engineering Department
University of Michigan
Ann Arbor, MI 48109

for the period:

May 1, 1991-September 30, 1995

19960103 215

REPORT DOCUMENTATION PAGE

Public reporting burden for this collection of information is estimated to average 1 hour per response, including the time for reviewing instructions, searching existing data sources, gathering and maintaining the data needed, and completing and reviewing the collection of information. Send comments regarding this burden estimate or any other aspect of this collection of information, including suggestions for reducing this burden, to Washington Headquarters Services, Directorate for Information Operations and Reports, 1215 Jefferson Davis Highway, Suite 1204, Arlington, VA 22202-4302, and to the Office of Management and Budget, Paperwork Reduction Project (0704-0188), Washington, DC 20503.

1. AGENCY USE ONLY (Leave blank)	2. REPORT DATE 12/20/95	3. REPORT TYPE AND DATES COVERED Final - 5/1/91-9/30/95

4. TITLE AND SUBTITLE
Theoretical and Experimental Studies of a Novel Accelerating Structure

5. FUNDING NUMBERS
ONR Contract
SFRC Number
N00014-91-J-1941

6. AUTHOR(S)
R. M. Gilgenbach and Y. Y. Lau

7. PERFORMING ORGANIZATION NAME(S) AND ADDRESS(ES)
Nuclear Engineering Department
University of Michigan
Ann Arbor, MI 48109-2104

8. PERFORMING ORGANIZATION REPORT NUMBER

9. SPONSORING/MONITORING AGENCY NAME(S) AND ADDRESS(ES)
Ballistic Missile Defense Organization
Innovative Science and Technology/
Office of Naval Research

10. SPONSORING/MONITORING AGENCY REPORT NUMBER

11. SUPPLEMENTARY NOTES

12a. DISTRIBUTION/AVAILABILITY STATEMENT
Approved for public release;
distribution is unlimited.

12b. DISTRIBUTION CODE

13. ABSTRACT (Maximum 200 words)

The major accomplishment reported herein is the invention of a two-beam accelerator, named "Twobetron" that was supported by this contract. A patent is being granted. This accelerator uses the power of an intense annular relativistic electron beam to drive a low current on-axis pencil beam to high energies for industrial and medical applications. For the purposes of this report, high energy is in the 1 to 10 MeV range rather than the GeV range in the high energy physics community. Summarized in this report are the concepts, theories, simulation results, studies of beam modulation, and initial experimental studies.

14. SUBJECT TERMS
Electron beams, accelerators, beam-breakup-instability

15. NUMBER OF PAGES
73

16. PRICE CODE

17. SECURITY CLASSIFICATION OF REPORT UNCLASSIFIED	18. SECURITY CLASSIFICATION OF THIS PAGE UNCLASSIFIED	19. SECURITY CLASSIFICATION OF ABSTRACT UNCLASSIFIED	20. LIMITATION OF ABSTRACT Unlimited

NSN 7540-01-280-5500

Standard Form 298 (Rev 2-89)
Prescribed by ANSI Std 239-18
298-102

i

Table of Contents

Distribution /

Availability Codes

Dist	Avail and / or Special
A-1	

Introduction

The major accomplishment reported herein is the invention of a two-beam accelerator, named "Twobetron" [1] that was supported by this contract. A patent is being granted [2]. This accelerator uses the power of an intense annular relativistic electron beam to drive a low current on-axis pencil beam to high energies for industrial and medical applications. For the purposes of this report, high energy is in the 1 to 10 MeV range rather than the GeV range in the high energy physics community.

Summarized below are the concepts, theories, simulation results, studies of beam modulation, and initial experimental studies. The details are given in the references. The ones supported by this contract are attached to the end of this Report.

Theory
Concept

In the Twobetron, an intense annular relativistic electron beam with current I_d travels down a series of pillbox cavities at radius r_0 to accelerate a pencil beam with current $I_s << I_d$. Both the driver beam (I_d) and the secondary beam (I_s) are modulated at a frequency w_0, the frequency of the TM_{020} mode of the cavity [Fig. 1]. The driver beam is always decelerated by the mode, by conservation of energy. Since the electric field of the TM_{020} mode has opposite polarity in the outer and the inner radius, this mode decelerates the annular beam and accelerates the

pencil beam if the beams enter the cavity in the same phase. As the driver beam loses energy and the pencil beam gains energy, however, the two beams will drift out of phase with one another, and acceleration will cease. This phase slippage has a simple cure [1]: At the locations where the bunches of both beams enter the cavity with the same phase, place the annular beam radius (r_o) outside the the field null (a) of the TM020 mode. When the bunches of both beams arrive at the cavity 180° out of phase, place r_o inside a. The radius modulation can be accomplished by varying the external solenoidal magnetic field. Figure 2 shows an example of acceleration of a test electron on the secondary beam from 700 keV to 5 MeV in approximately one meter of accelerating structure; the driver beam is available from MELBA [3].

The energy gain per cavity by the secondary beam in a twobetron is

$$< E_s >= (16.3 \, keV) \times Q \times (I_d \, / \, 1kA) \times (\Delta \, / \, a). \tag{1}$$

where Q is the cavity quality factor of the TM020 mode and Δ is the amplitude in the modulation of the primary beam radius. The transformer ratio, R, which is the ratio of the energy gain in the secondary beam to the energy loss in the primary beam, is

$$R = 0.803(a \, / \, \Delta). \tag{2}$$

The maximum amount of secondary beam current, I_s, that can be accelerated is limited

$$I_s < \frac{I_d}{2R}. \tag{3}$$

Beam Loading

With radius modulation, the driver beam must necessarily pass through the field null of the TM_{020} mode. When this occurs, the driver beam cannot perform work on the mode ($J*E=0$), whereas the secondary beam does work against the mode, causing the secondary beam to decelerate. By relaxing the assumption of a test particle on the secondary beam, we study the effect of beam-loading. The result is shown in Fig. 3 where we see that, as I_s is increased, the final beam energy in 90 cm is reduced.

Beam Breakup Instability

Another theoretical issue that has been addressed is the primary beam instabilities. A beam with sizable current traveling down a series of pill box cavities is vulnerable to a host of instabilities. Of most concern is the beam breakup instability (BBU). However, we discovered [4] that annular beams may be up to 6 times more stable than pencil beams against the deflecting dipole TM_{110} mode. That is, the annular beam can carry 6 times as much current as a pencil beam and suffer the same BBU growth. For the parameters of the MELBA example, the number of e-folds for BBU growth is 1.8 for a 500 ns beam [Fig. 2].

Other beam instabilities such as the Robinson instability and wakefield effects do not pose a threat to the Twobetron concept [5].

5

Simulation

Several primary beam issues have been addressed with simulation. In the simulation, 40 cavities of the accelerating structure have been simulated with the MAGIC code, which is a 2.5 dimensions, fully relativistic, electromagnetic particle-in-cell code [6]. In all cases, the MELBA parameters [Fig. 2] were used. The first case involved the beam traveling down the accelerating structure to test that the modulation is preserved, and that no virtual cathodes were formed. As can be seen from Fig. 4, the beam travels the length of the structure with no disruption and the current modulation remains intact. If we look at the cavity fields, however, we see that the structure is experiencing serious mode competion with both the TM_{010} and TM_{030} competing with the desired TM_{020} mode [Fig. 5]. This agrees with intuition since the beam is placed near the field null of the TM_{020} mode, which approximately corresponds to the maximum of the TM_{030} mode. Clearly, mode competion is a challenging issue to the Twobetron concept. Furthermore, the phase space plots of the beam's energy [Fig. 6] show that the driver beam is both accelerated and decelerated by the structure. Further tests show that the twobetron, in its present configuration is a traveling wave device. This implies that a traveling wave formulation must be developed for the Twobetron, or work must be done to isolate the cavities electromagnetically [5].

Driver Beam Modulation

Simulation was also performed on primary beam modulation for the MELBA example. The geometry [Fig. 7] is similar to the existing methods of intense beam modulation [7] used in relativistic klystron amplifiers [RKA's]. For a low current driver beam (500A), the modulation was on the order of 30% [Fig. 8]. This was found to agree with theory as there is simply not enough space charge in the beam for full modulation at convenient levels of external rf drive. We therefore decided to study the effect of adding a feedback loop to increase beam modulation [Fig. 9]. This concept is similar to experiments performed recently at Phillips Laboratory [8] on injection-locked Relativistic Klystron Oscillators (RKO), except that the Phillips Lab experiment utilized feedback from the cavities being close to each other for effective electromagnetic coupling.

We analyzed the above-mentioned injection-locked RKO with a lumped circuit model of the cavities [9], including the finite travel time for the beam between the cavities and the phase behavior of the fields in the cutoff region. Even though the model is fairly simple, it showed excellent agreement with experimental results[8]. The major conclusion is that coupling could destabilize the system to provide current modulation in a far shorter drift space (13 cm vs. 30 cm) than a conventional RKA with a lower gap voltage on the booster cavity, thus avoiding breakdown and virtual cathode. The drawback, when applied to the twobetron concept, is that there is a current threshold for the operation in the injection-locked mode, which for the parameters studied was 7.2kA. Such a high current may make the primary beam vulnerable to BBU if the accelerating structure is excessively long.

Experiments and Simulations

Beam Transport simulations

The SLAC Electron Trajectory Program[10] (EGUN)was used in beam transport studies to determine the alpha spread of an annular beam as well as beam transport characteristics. For the first set of measurements the 4.5 cm radius cathode was modeled. The parameters used for EGUN simulations were as follows: cathode voltage 750 keV, diode radius 20 cm, drift tube radius 7.5 cm, A-K gap 8.2 cm. The cathode was modeled to emit between 4.25 and 4.75 cm. This experiment was run using glyptal enamel to prevent emission from other surfaces. In the computer simulation the first 2 cases used a magnetic field similar to that measured in the experiment. Case 1 results are shown in figure 10. These show a transported current of 3.2 kA with 4.07 kA emitted from the cathode. As figures 10 and 11 show, there is some beam scraping going through the anode aperture. The average beam alpha (Vperp/Vparallel) was determined to be approximately 0.45. Case 2 shown in figure 11 shows the same model with a grounded plane across the anode surface. This plane simulates aluminized mylar used in the experiment. With the grounded plane, only 2.28kA of current is seen in the drift tube as opposed to 3.2 kA of case 1. But as can be seen from EGUN simulations the beam is much more focused in the second case. The beam needs to be focused to pass through accelerating cavities with slots that are 0.5 cm wide. The average beam alpha for the second cases was 0.45, the same as case 1. Experimentally currents ranging on the order of 1.8kA were measured using the configuration of case 2.

A more realistic model of a transport experiment is shown in figure 12. This model used a cathode that emitted at 3.5 +/- 0.25 cm. The cathode emitted into a 4 inch drift tube after passing through the diode. The A-K gap was set to 11 cm. The Magnetic field of the diode was approximately 1kGauss and the drift tube raises the magnetic field to 2 kGauss. The diode current is 2.8kA which is fully transported down the drift tube in the simulation. The average beam alpha measured was 0.6. In experimental comparison 2kA was transported through the drift tube, but the initial diode current was on the order of 5-10kA.

One final case shown in figure 13 shows the same parameters as in figure 12, but the cathode is now modeled with a radius of 2.25 cm with an emitting surface of 2.0 to 2.5 cm. The emitting surface is also flat vs curved as in the other cathodes. The transported tube current produced in EGUN showed 1.84kA transported. The average beam alpha in the simulation was 0.2. Experimentally, the tube current at 2kGauss has been measured to range between 1 and 3 kA, but diode current ranges between 6 and 10 kA.

Experimental Results:

Accelerating Cavity Design and Cold Tests

Using parameters listed in [1], accelerating cavities were designed. Since the RF electric field null associated with an axial electric field of the TM_{020} cavity mode occurred at 3.146 cm [1], cavity slots were placed at 3.35 +/- 0.25 cm. The cavity radius was 7.24cm. The cavity was 1 cm thick. Dimensions of the accelerating cavity are shown in figure 14. A different cavity without slots was

also constructed. Cold tests of the cavity with slots resulted in frequency measurements of figure 15. The cold test utilized an HP 8510 Network analyzer. Port one of the two port network was connected to a loop antenna placed inside one of the slots. A monopole antenna was placed in the center of the cavity. The first peak in Figure 15 occurs at 3.47GHz. This result can be accounted for by one of two modes, either the TM_{21} (3.39 GHz) or the TM_{02} (3.64 GHz). The second peak occurs at 4.0 GHz; this is due to the TM_{31}(4.21 GHz). And the third peak occurs at 4.39GHz which is due to the TM_{12} mode. The TM_{02} mode had a Q of 11. The TM_{31} mode appeared dominant with a Q of 80. This could be due to the design with three slots.

The cavity without slots for a beam was built with two loop antennas placed at the radius of the beam slots (r=3.15 cm). Port one of the network analyzer was connected through a power divider to the two antennas. A monopole antenna was placed in the center of the cavity and connected to port two of the network analyzer. Figure 16 shows the results. The TM_{02} mode demonstrated a weak response and occurred at 3.76GHz, but the dominant response was due to the TM_{41}(5.004GHz) peak which occurred at 4.88 GHz.

Annular e-Beam Transport Experiments:

Transport experiments have been conducted using three different cathodes. The cathode radii are 2.25cm +/-0.25 cm, 3.55cm +/- 0.25 cm, and 4.5cm+/-0.25 cm. Two cathodes are shown in figure 17. Initial experiments were conducted with an experimental configuration as shown in figure 18 (without the brass cavities). Experiments used a 6 inch drift tube with a graphite collector to measure transported current. A piece of aluminized mylar was placed in the anode aperture to give better results (EGUN simulations showed this effect). Experimental parameters are listed in figure 19 [16]. Using the cathode with a radius of 4.5cm and an empty drift tube, measurements were made; this was followed by placing a brass plate with three slots (radius 2.15cm+/-0.25 cm) in the drift tube between the anode and the graphite plate. Data recorded are shown in figures 20 and 21. The brass plate was replaced by a pillbox cavity with three slots (radius 2.25cm+/- 0.25 cm) for measurements recorded in figure 22. Two pillbox cavities were use to measure transported current in figure 23. Without placing anything in the drift tube, the maximum transported current was approximately 1.8kA. With a brass plate, the maximum transported current was 900A at a magnetic field of 3kGauss. Placing a pillbox cavity in the drift tube reduced the maximum transported current to 680A at 3.7kGauss. With two pillbox cavities, the maximum transported current was less than 300A at 3.9kGauss. Figure 24 shows the results of one MELBA shot with a pillbox cavity in the drift tube.

11

The cathode with a 3.55cm radius and the cathode with the 2.25 cm radius were used with a 4 inch drift tube for transport current measurements. Figure 25 shows the results utilizing the 3.55 cm radius cathode. These measurements did not use aluminized mylar. Figure 26 shows the transported current using the 2.25 cm radius cathode.

Figure 27 shows the final, proposed Twobetron experimental design showing the orientation of the accelerating cavities with the primary and secondary beams.

Conclusions

The Twobetron concept is a viable, intriguing candidate for industrial and medical accelerators. While challenges exist, the potential to upgrade pulsed power systems and develop new compact accelerators argues for the continued development of this two-beam accelerator scheme.

References

[1]*   Derbenev et al., Phys. Rev. Lett. 72, 3025 (1994).

[2]   Ya. S. Derbenev, Y. Y. Lau, R. M. Gilgenbach, "Two Beam Particle Acceleration Mehtod   and Apparatus", submitted to US Patent and Trademark Office, Feb. 18, 1994, UM File   #916. Notice of Allowability issued by Us Patent and trademark Office on July 24, 1995.

[3]   R. M. Gilgenbach et. al., in Digest of Fifth Pulse Power Conference (IEEE, New York, 1985) p. 126.

[4]*   Lau and Luginsland, J. Appl. Phys. 75, 5877 (1993).

[5]*   Lau et al., AIP Conf. Proc. 335, "Advanced Accelerator Concepts"' Ed.: P. Schoessow,   p. 451 (1995).

[6]   Goplen et. al. Computer Phys. Comm. 87, 1, 54 (1995).

[7]   Friedman et. al., J. Appl. Phys. 64, 3353 (1988).

        Friedman et. al., Rev. Sci. Instrum. 61, 171, (1990).

[8]   Hendricks et al., Phys. Rev. Lett. (in press, 1996).

[9]*   Luginsland et al., Special Issue on HPM, IEEE Trans. Plasma Sciences (in press, 1996).

[10]   William B. Herrmannsfeldt, Electron Trajectory Program, Stanford Linear Accelerator Center, 1979

* Attached to the end of this Report.

<u>Patent</u>:

Ya. S. Derbenev, Y. Y. Lau, R. M. Gilgenbach, "Two Beam Particle Acceleration Method and Apparatus", submitted to US Patent and Tademark Office, Feb. 18, 1994, UM File # 916. Notice of Allowabilty issued by US Patent and Trademark Office on July 24, 1995.

* *

The following refereed papers, conference procedings papers, and abstracts, were supported by the present SDIO/IST/ONR contract:

* *

<u>Refereed archival journal articles</u>:

Y. Y. Lau and J. W. Luginsland, "Beam Breakup Instability in an Annular Electron Beam," J. Appl. Phys. 74, 5877 (1993).

P. Menge, R. M. Gilgenbach, Y. Y. Lau, and R. Bosch, "Beam Breakup Growth Reduction Experiments in Long Pulse Electron Transport," J. Appl. Phys. 75, 1258 (1994).

Ya. S. Derbenev, Y. Y. Lau, and R. M. Gilgenbach, "Proposal for a Novel Two-Beam Accelerator", Phys. Rev. Lett. 72, 3025 (1994).

J. W. Luginsland, Y. Y. Lau, K. Hendricks, and P. D. Coleman, "A Model of Injection Locked Relativistic Klystron Oscillator", Special Issue on High Power Microwaves, IEEE Trans. Plasma Sciences (to be published, 1996).

P. R. Menge, R. M. Gilgenbach, and Y. Y. Lau,"Experimental Reduction of Beam-Breakup Instability Growth by External Cavity Coupling in Long-Pulse Electron Beam Transport", Physical Review Letters <u>69</u> 2372 (1992)

P.R. Menge, R. M. Gilgenbach, and R. A. Bosch, "Microwave Growth from the Beam Breakup Instability in Long-Pulse Electron Beam Experiments," Applied Physics Letters, <u>61</u> 642 (1992).

R. A. Bosch, P. R. Menge, and R. M. Gilgenbach, "The Beam Breakup Instability in Quadrupole and Solenoidal Electron Beam Transport Systems," Journal of Applied Physics, <u>71</u> (1992).

Conference Abstracts:

J. W. Luginsland, Y. Y. Lau, and R. M. Gilgenbach, "Beam breakup in an Annular Beam", Bull. Am. Phys. Soc. 38, 2074 (1993).

R. M. Gilgenbach, Y. Y. Lau, Y. S. Derbenev, J. Luginsland, J. M. Hochman, W. T. Walter, and C. H. Ching, "Design Studies of a Novel Two-Beam Accelerator", Bull. Am. Phys. Soc. 39, 1555 (1994).

Full Conference Papers:

Y. Y. Lau, Y. S. Derbenev, R. M. Gilgenbach, J. Hochman, J. Luginsland, M. Walter, and C. H. Ching, "Novel, Compact, Two-Beam Accelerator",
in Proc. 10th International Conference on High Power Particle Beams, p. 37 (1994).

Y. Y. Lau, Y. S. Derbenev, R. M. Gilgenbach, J. Luginsland, J. Hochman, and M. Walter, "A Novel, Two- Beam Accelerator (Twobetron)", AIP Conf. Proc. # 335, "Advanced Accelerator Concepts", Ed. : P. Schoessow, p. 451 (1995).

Personnel Involved in This Research
1) R. M. Gilgenbach, Professor
2) Y. Y. Lau, Professor
3) Ya. S. Derbenev, Visiting Research Scientist
4) John Luginsland, Graduate Student (Theory)
5) Jonathan Hochman, Graduate Student (Experiment)
6) Mark Walter, Graduate Student (Experiment, received Ph.D. in 1995)
7) Peter Menge, Graduate Student (Experiment, received Ph.D. in 1993)
8) R.A. Bosch, Research Associate
9) C.H. Ching, (Experiment, received Ph.D. in 1994)

Honors and Awards

Y. Y. Lau received the Excellence in Research Award from the University of Michigan Nuclear Engineering Department in January 1994. Professor Lau was appointed Associate Editor of Physics of Plasmas, effective January 1994. R.M. Gilgenbach received the Research Exclellence Awards from the Engineering College and the Nuclear Engineering Department in 1993.
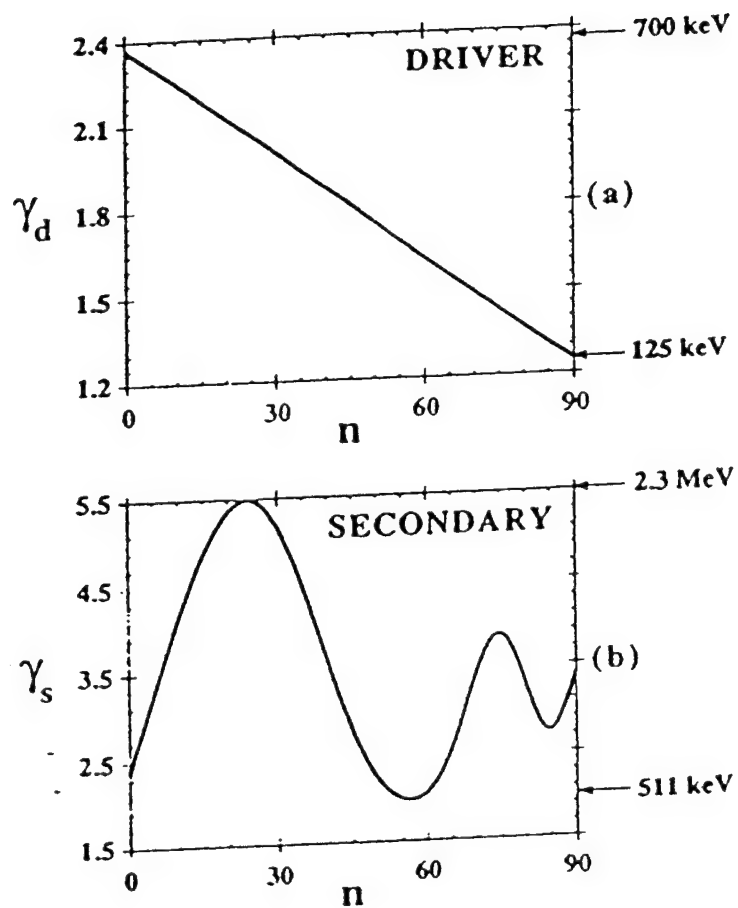
FIG. 1 Evolution of the relativistic mass factors when the driver beam radius r_0 is a constant: (a) the driver beam, (b) the secondary beam. Phase slippage prohibits continual acceleration of the secondary beam.
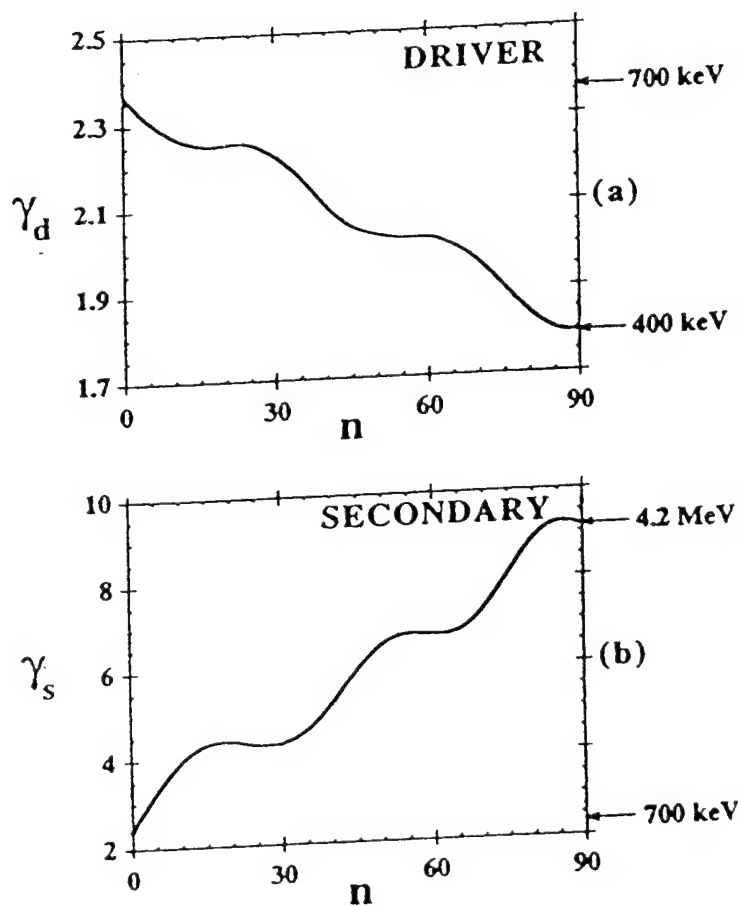
FIG. 2 Evolution of the relativistic mass factors when the driver beam radius r_0 is modulated to compensate phase slippage: (a) the driver beam, (b) the secondary beam.
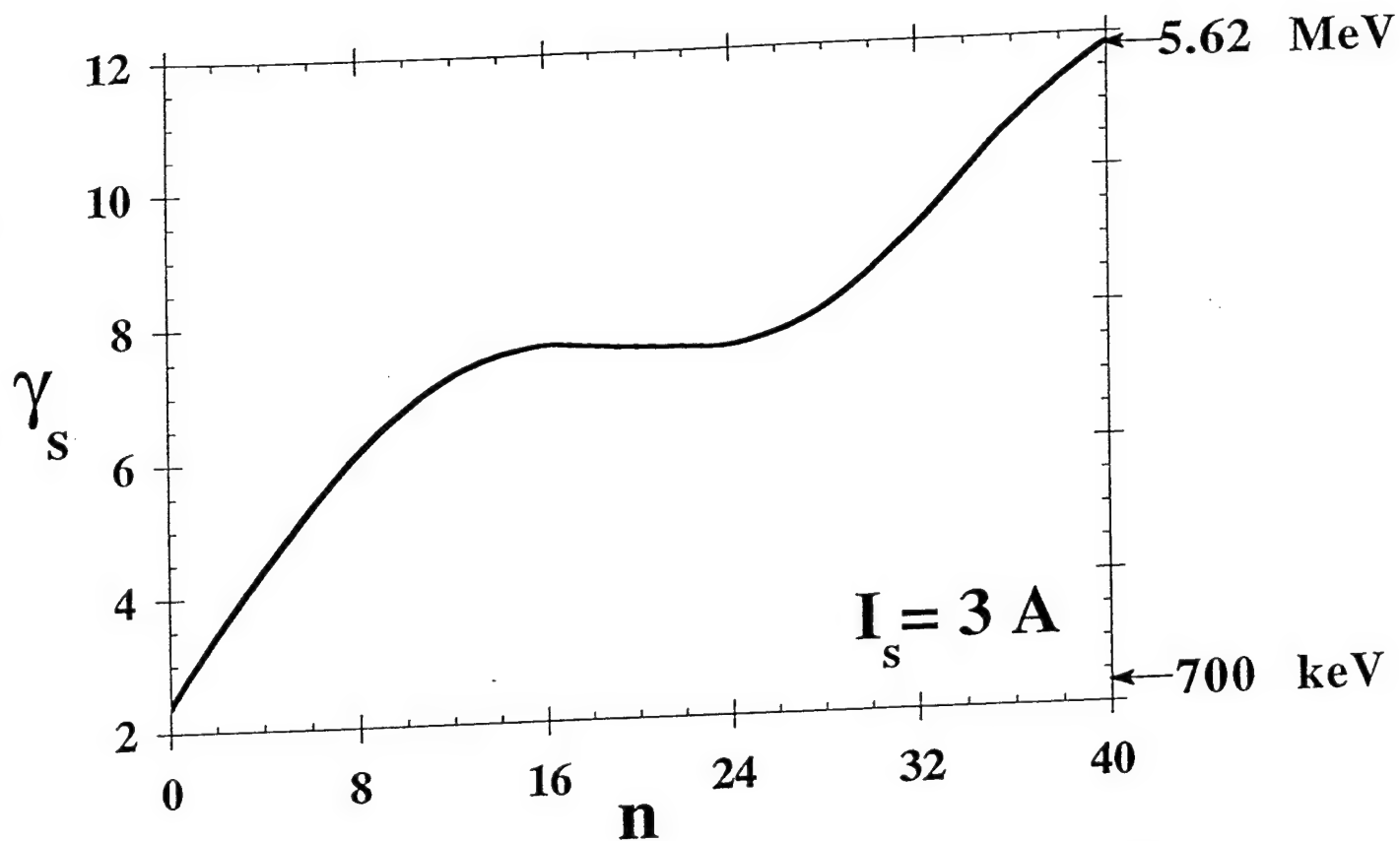
18
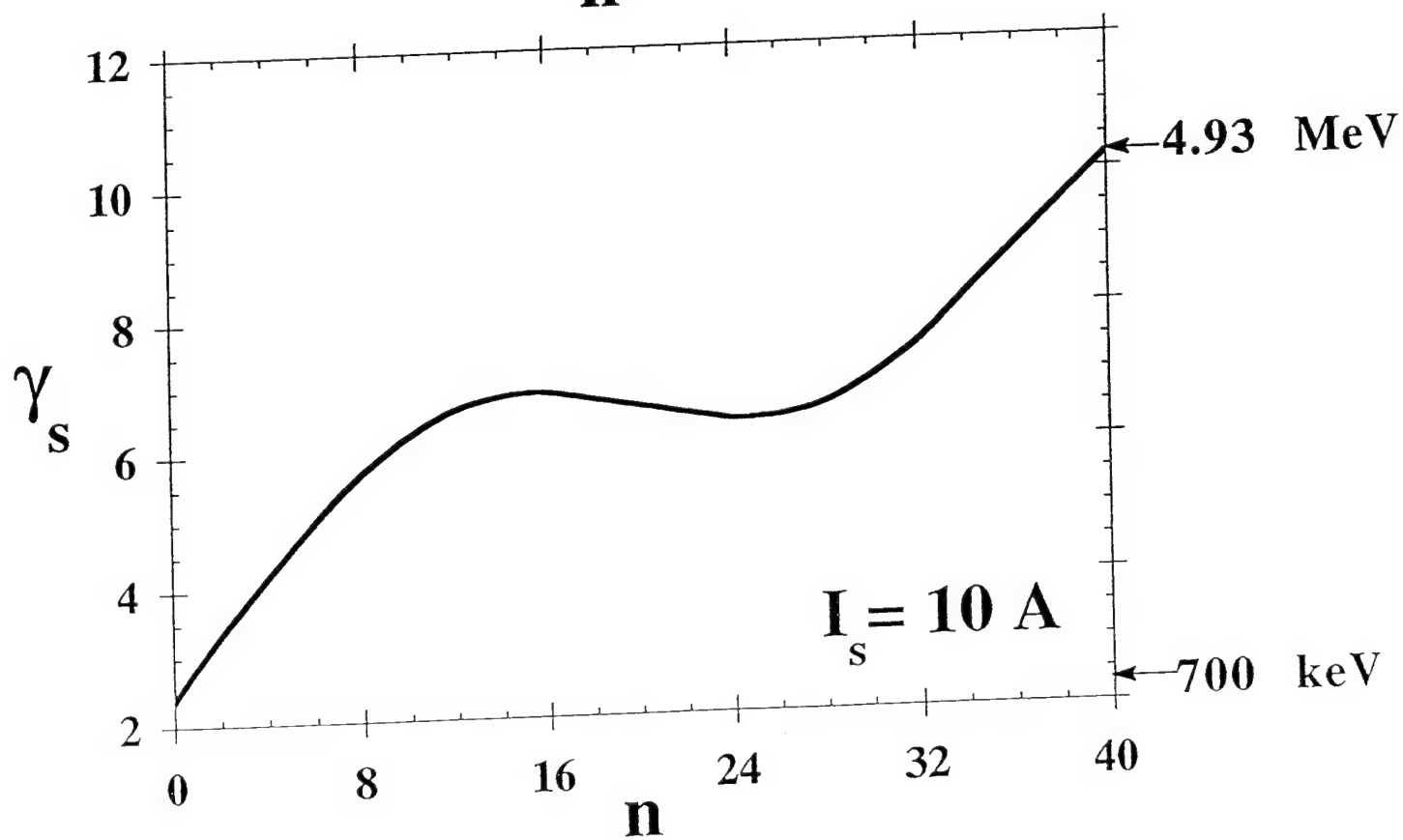
Fig.3
19

MAGIC VERSION.   DATE. Sep 15 1994
SIMULATION. TWOBETRON ACC. STRUCTURE

TRAJECTORY PLOT OF ELECTRON
FROM TIME 1.798E-09 SEC TO 1.800E-09 SEC

Fig. 4

20
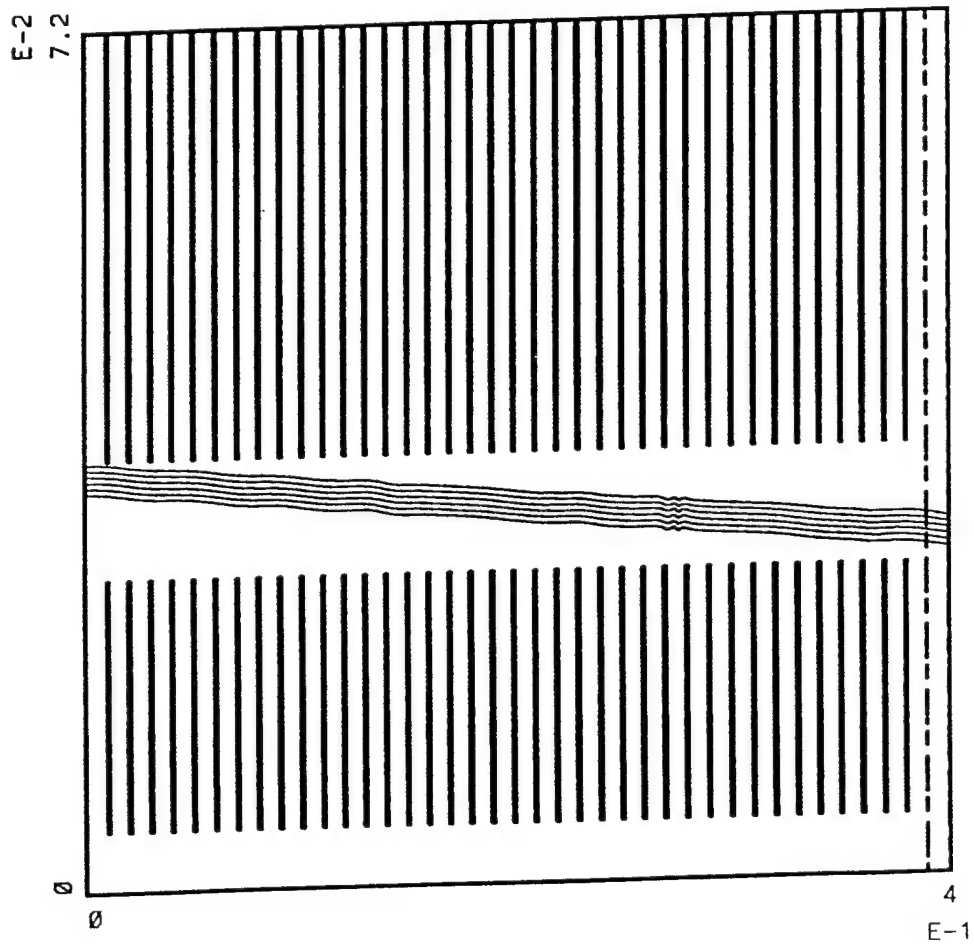
MAGIC VERSION,   DATE, Sep 15 1994
SIMULATION, TWOBETRON ACC. STRUCTURE

TIME HISTORY PLOT 3
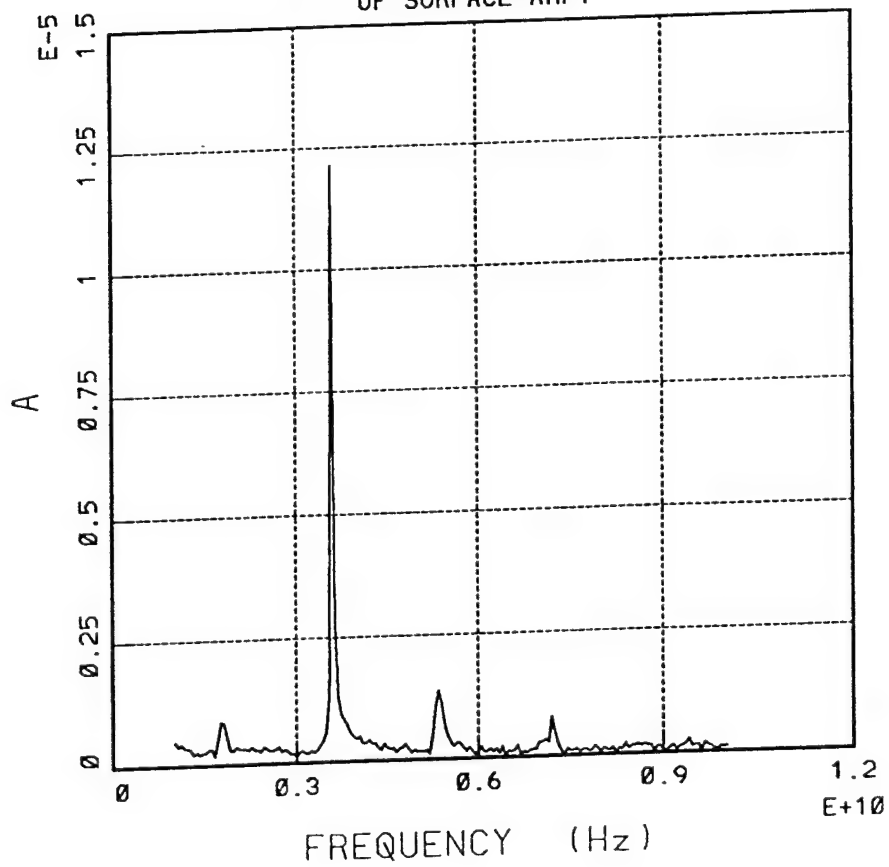MAGNITUDE OF FFT OF CURRENT
OF SURFACE AMP1

Fig. 5 a

21

MAGIC VERSION.   DATE. Sep 2 1994
SIMULATION. TWOBETRON ACC. STRUCTURE

TIME HISTORY PLOT 6
MAGNITUDE OF FFT OF E1 COMPONENT
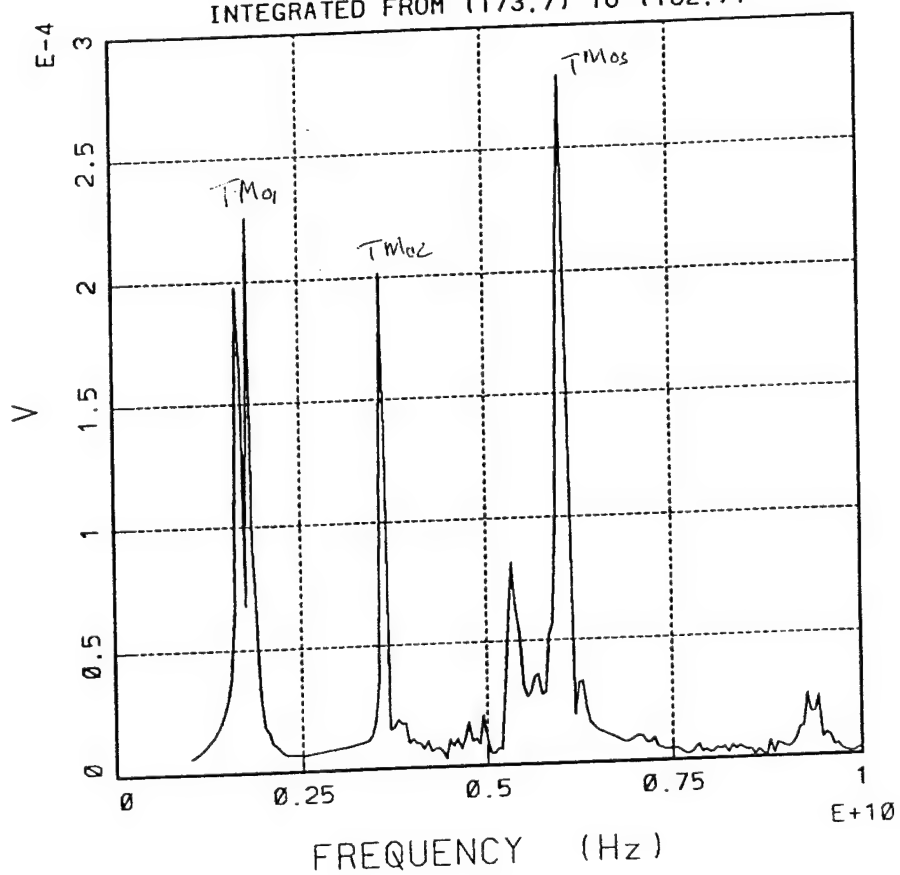INTEGRATED FROM (173.7) TO (182.7)

Fig. 5b

MAGIC VERSION.   DATE. Aug 3 1994
SIMULATION. TWOBETRON ACC. STRUCTURE

PHASE-SPACE PLOT OF PZ VS. Z AT TIME. 6.00E-10 SEC
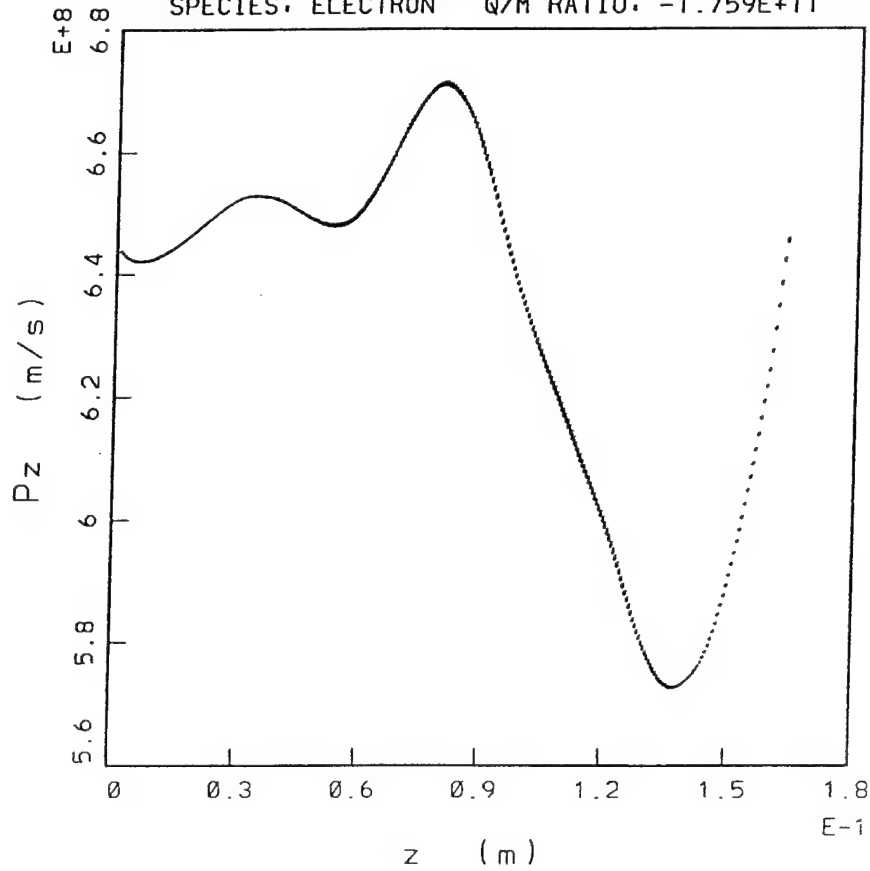SPECIES. ELECTRON   Q/M RATIO. -1.759E+11

Fig. 6

MAGIC VERSION.   DATE. Jan 9 1995
SIMULATION. SELF-MODULATING CAVITY

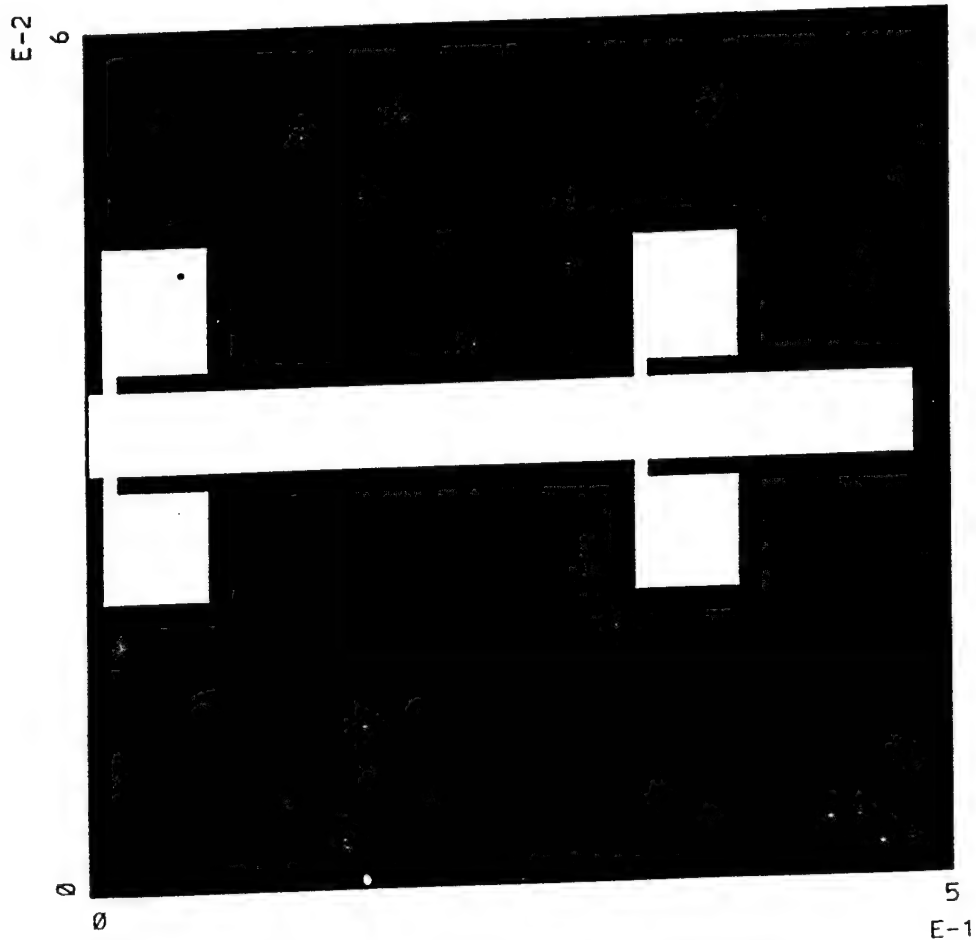VIEW OF GRID. CONDUCTORS. AND SYMMETRY BOUNDARIES

Fig. 7

24

MAGIC VERSION.   DATE. Sep 21 1994
SIMULATION. TWOBEAM ACCEL. MODULATING CAVITY
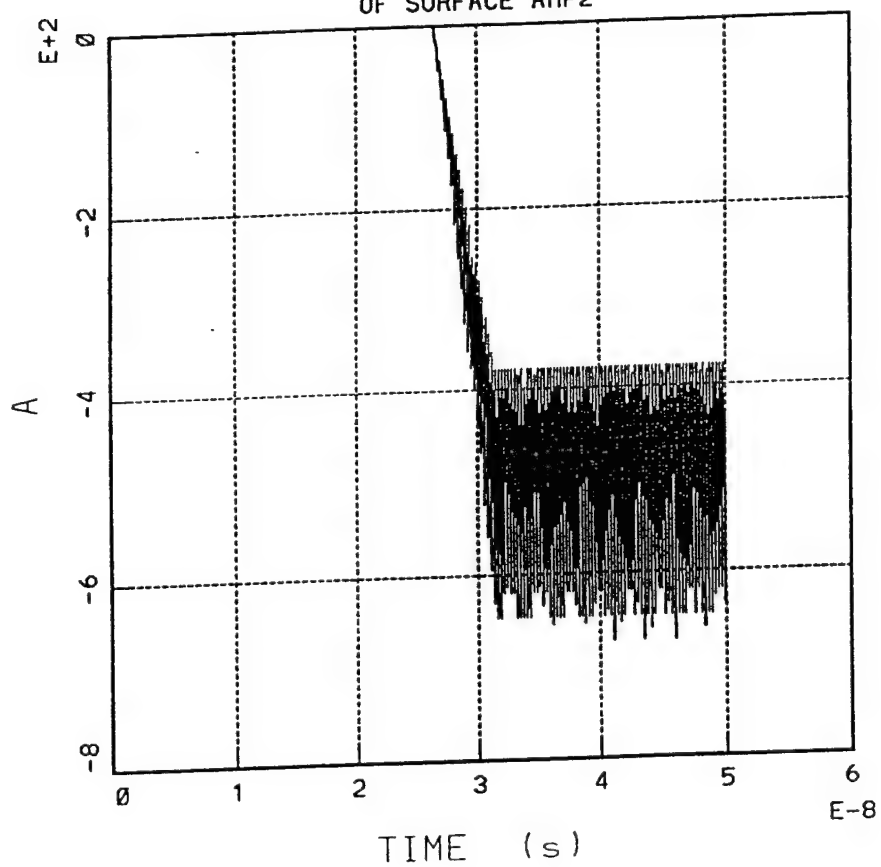
TIME HISTORY PLOT 5
CURRENT
OF SURFACE AMP2

Fig. 8

MAGIC VERSION.   DATE. Jan 10 1995
SIMULATION. SELF-MODULATING CAVITY

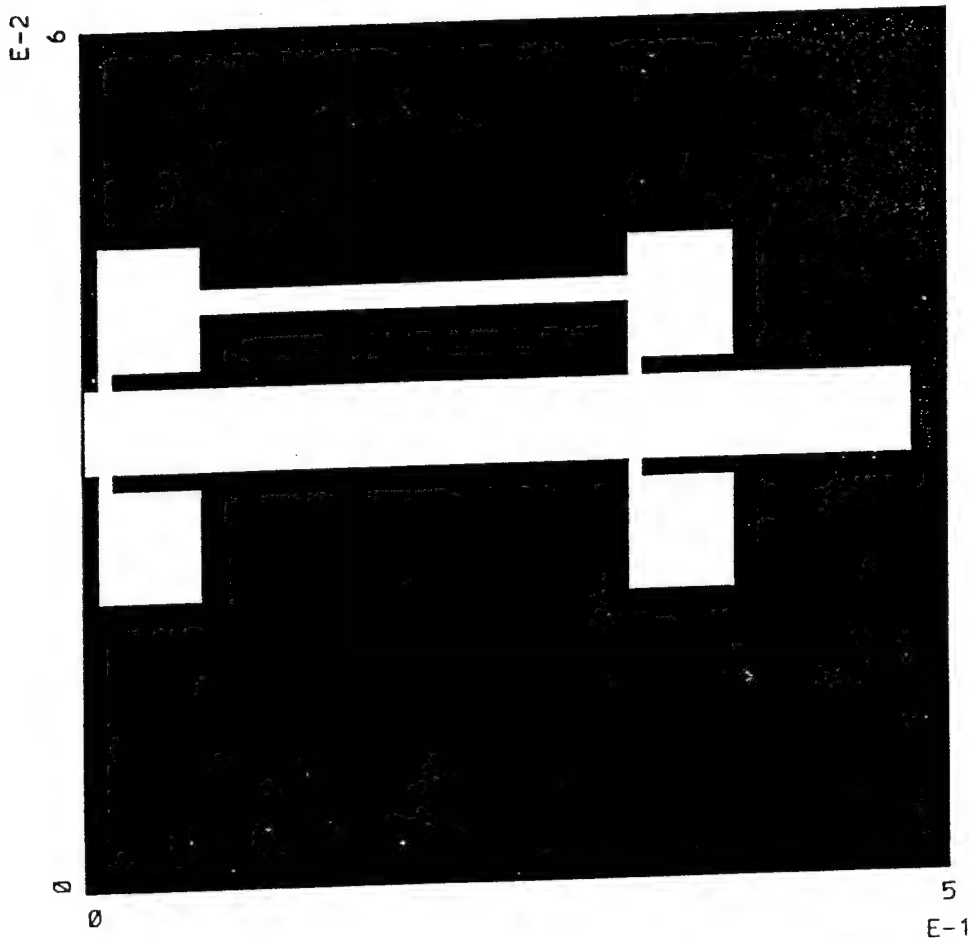VIEW OF GRID. CONDUCTORS. AND SYMMETRY BOUNDARIES

Fig. 9

RKO ~ PRKO ~ PRKA

Geometry

26

EGUN CASE 1: Low diode B field, no foil

Figure 10
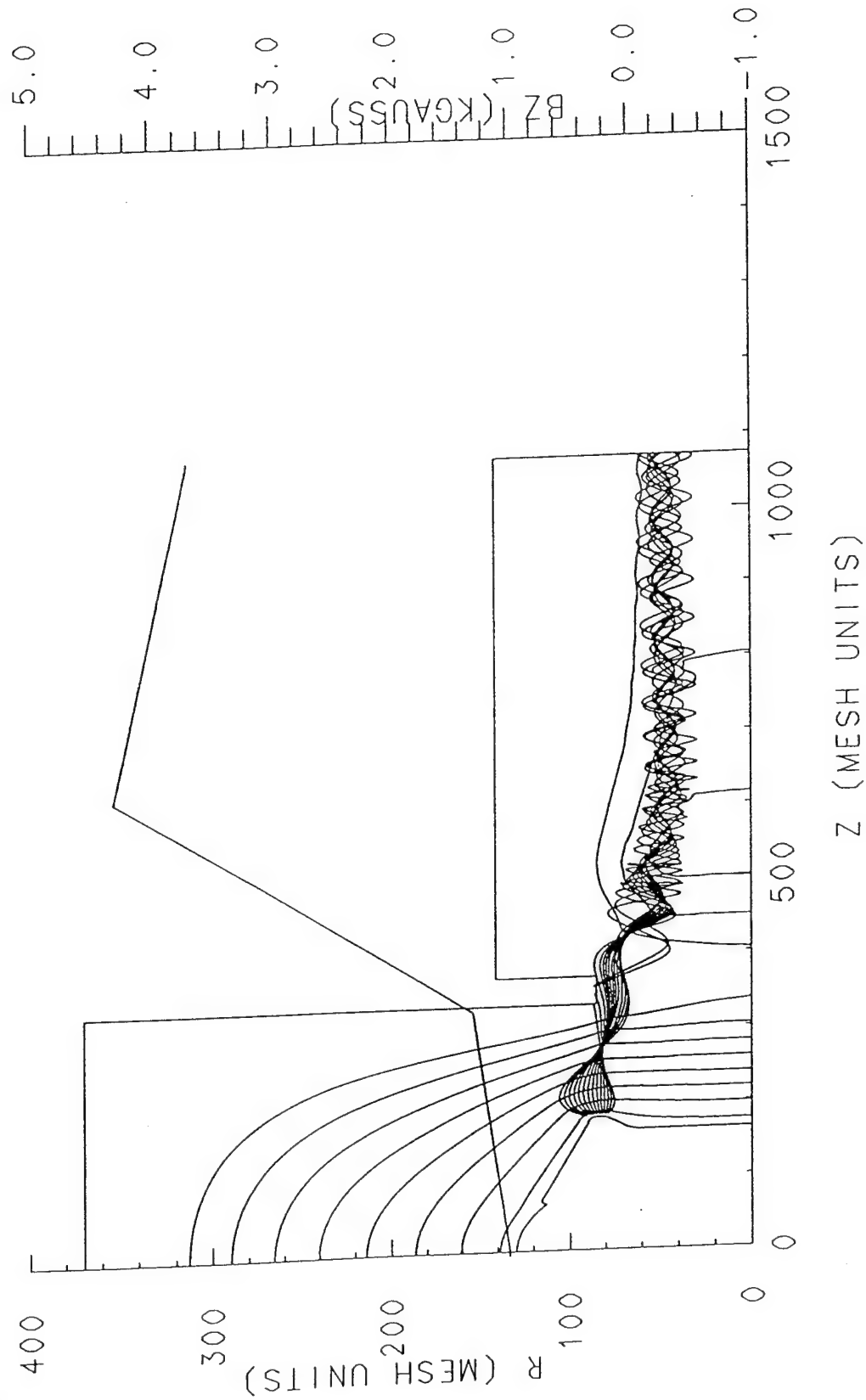
The University of Michigan

EGUN CASE 2: Low diode B field, anode foil

Figure 11

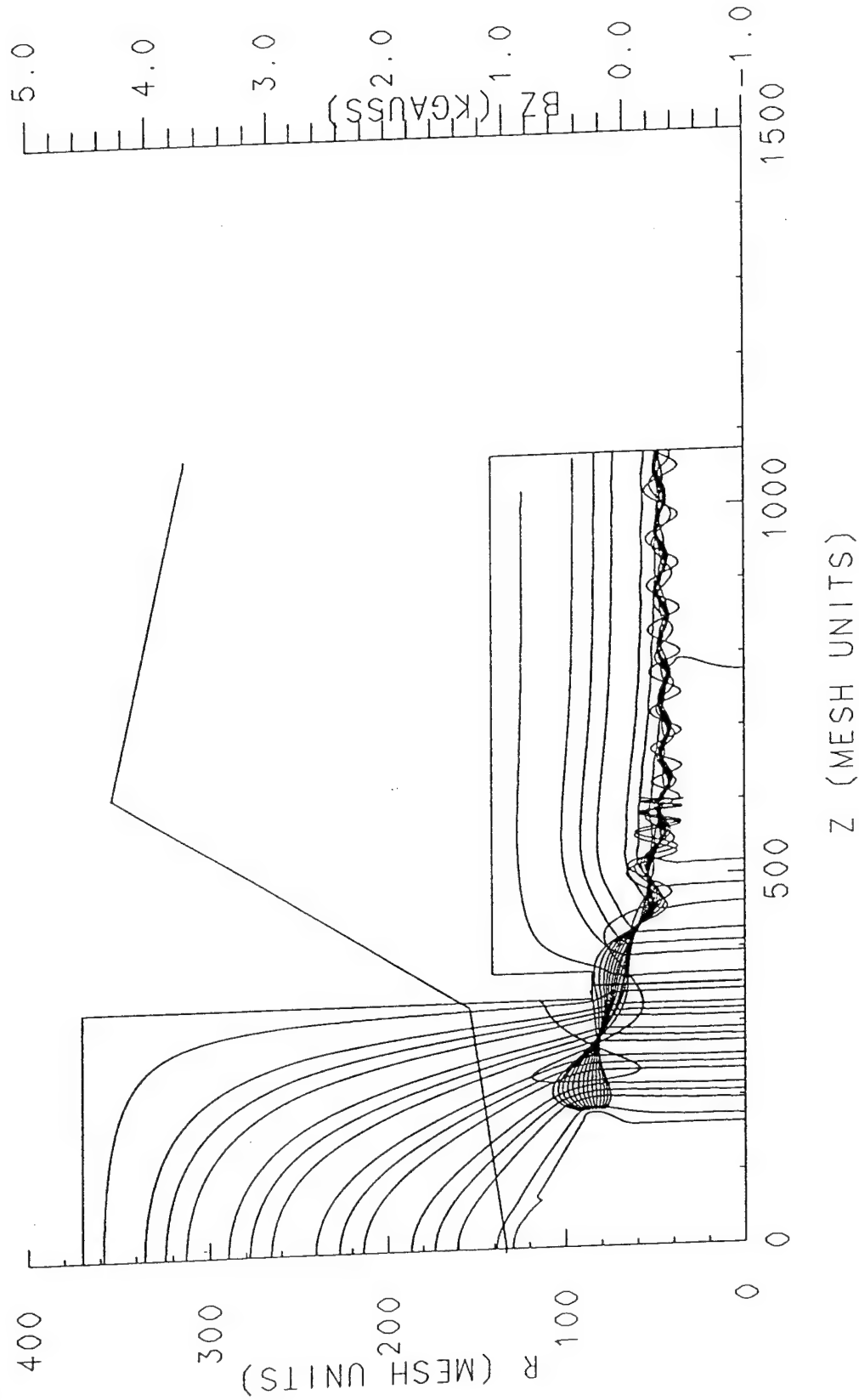The University of Michigan

EGUN CASE : Varying B-field (to 2kGauss)
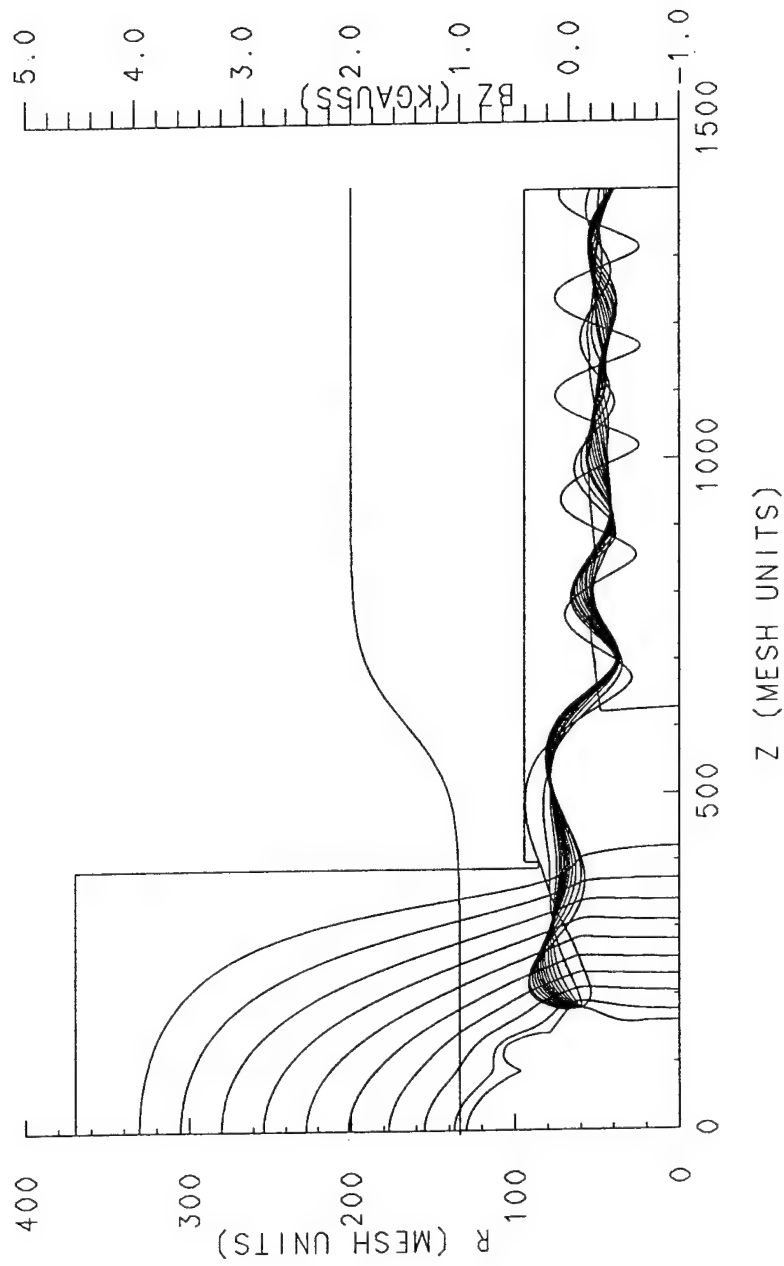
Figure 12

The University of Michigan

29

EGUN CASE: Varying B-field (to 2kGauss)
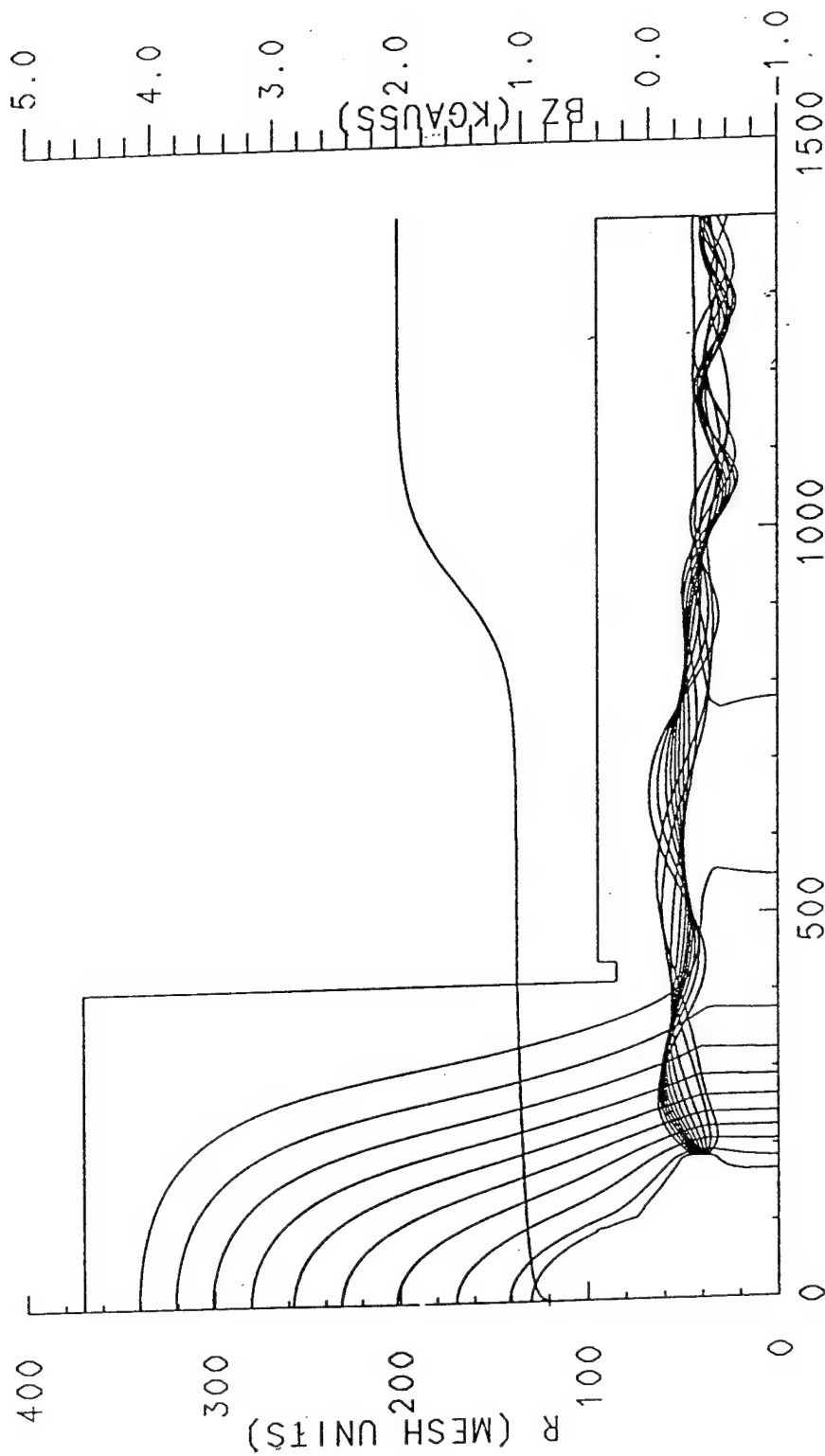
Figure 13

The University of Michigan

Cavity End plate

14.6 cm

.06cm

14.48 cm

.06 cm

0.16 cm

0.32cm

a=3.1cm
b=3.6cm

a

b
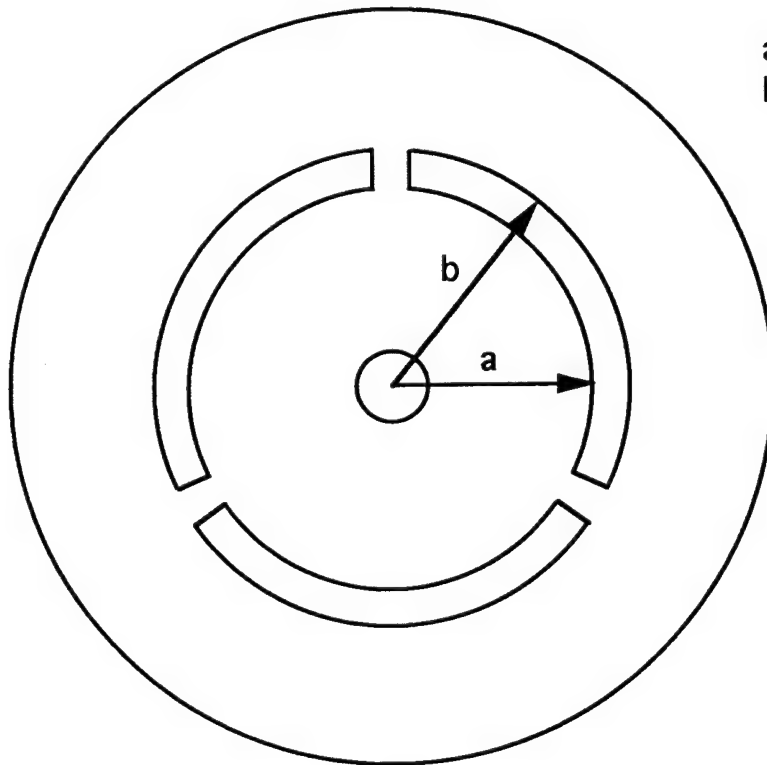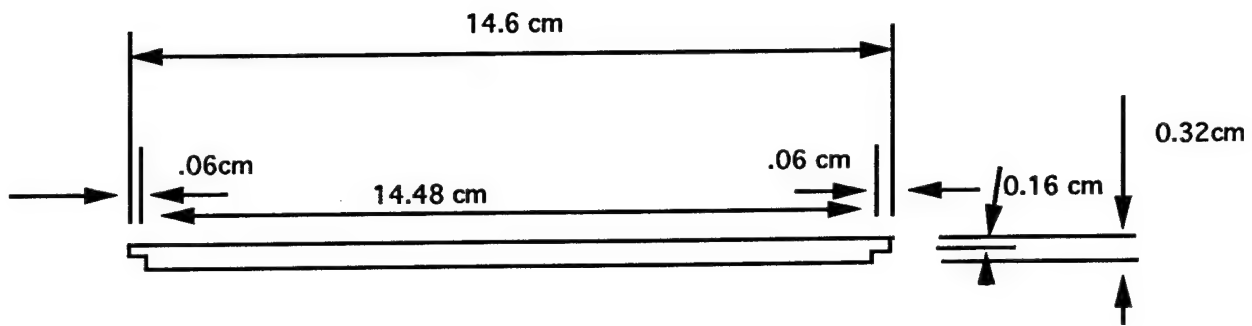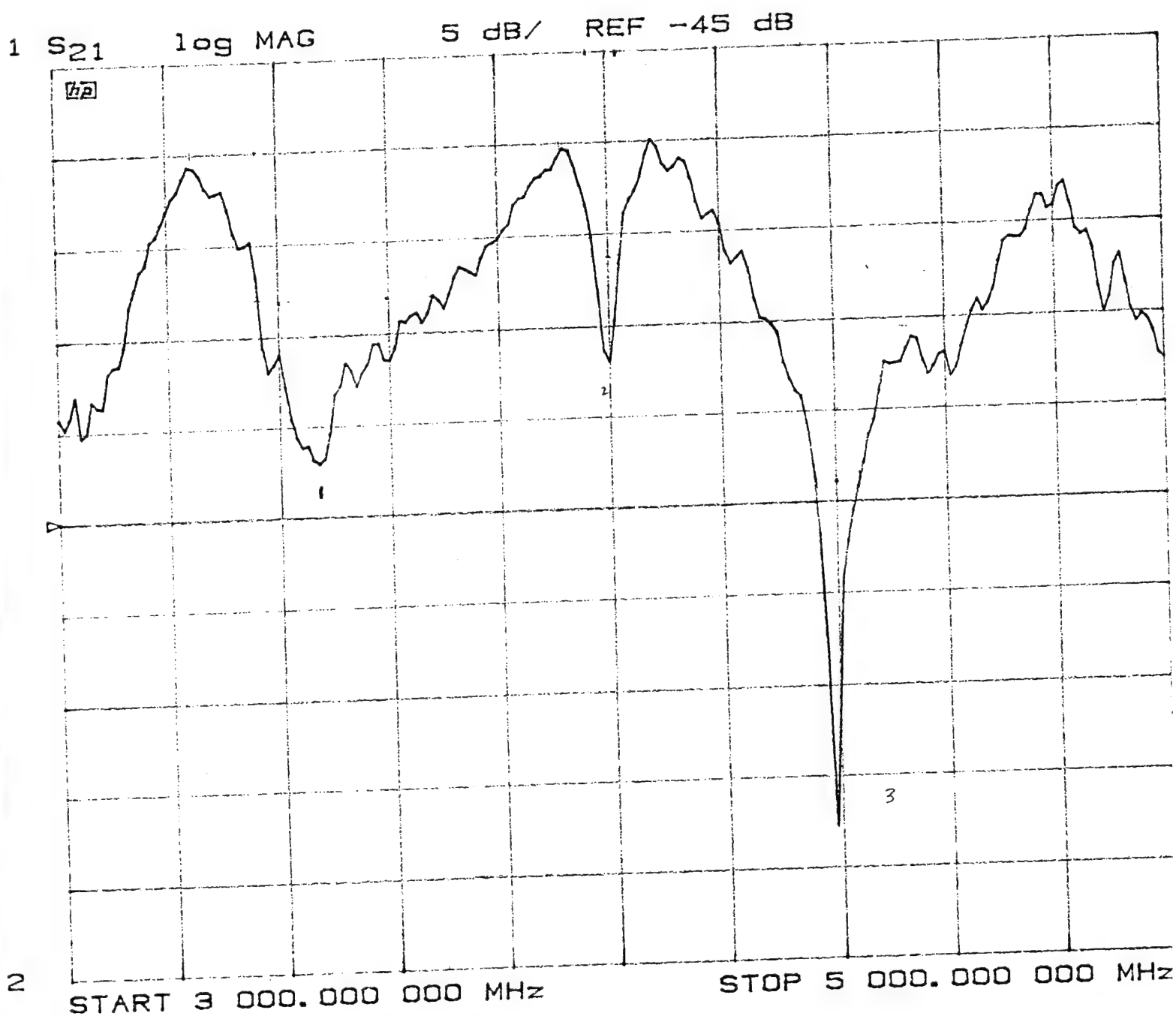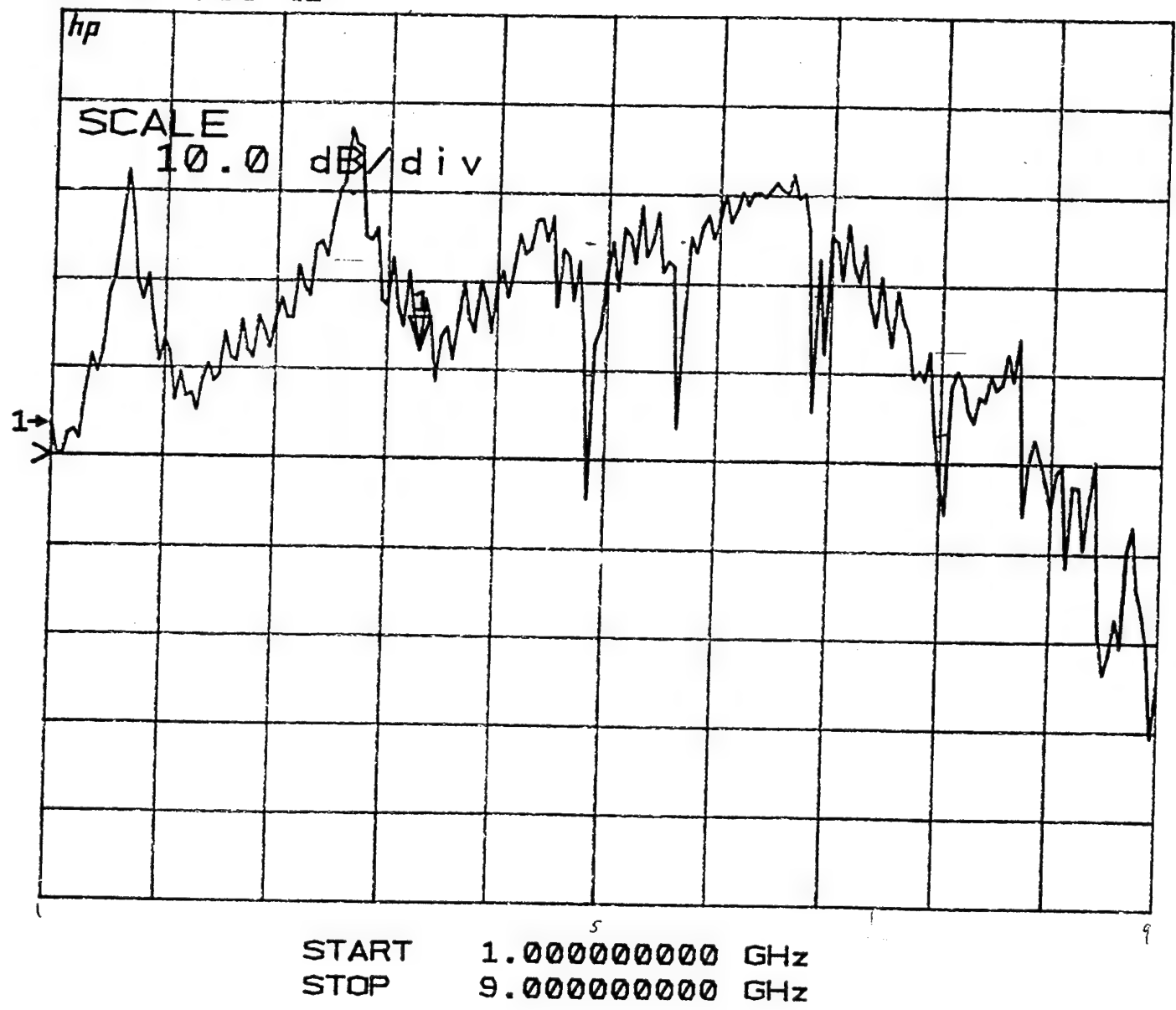
Figure 14

Figure 15

Figure 16

Cathode tips:

Figure 17

34

Figure 18

vacuum

Pearson coil

solenoid field windings

Brass cavities with slots

Graphite collector

diode coils

cathode

Aluminized mylar

35
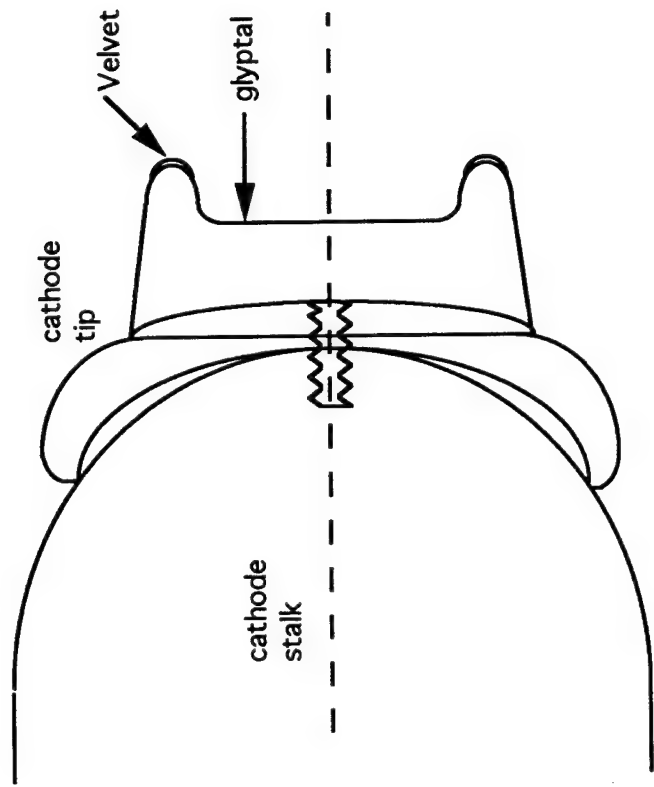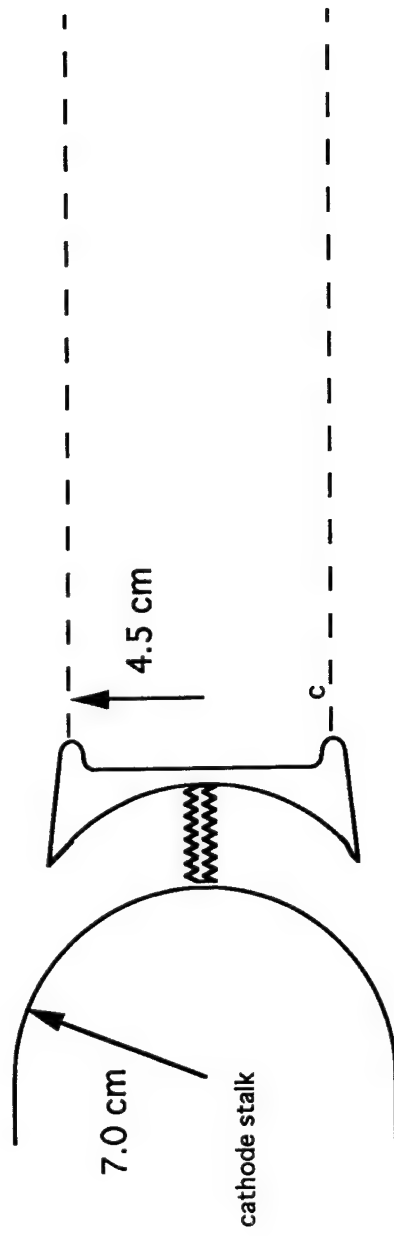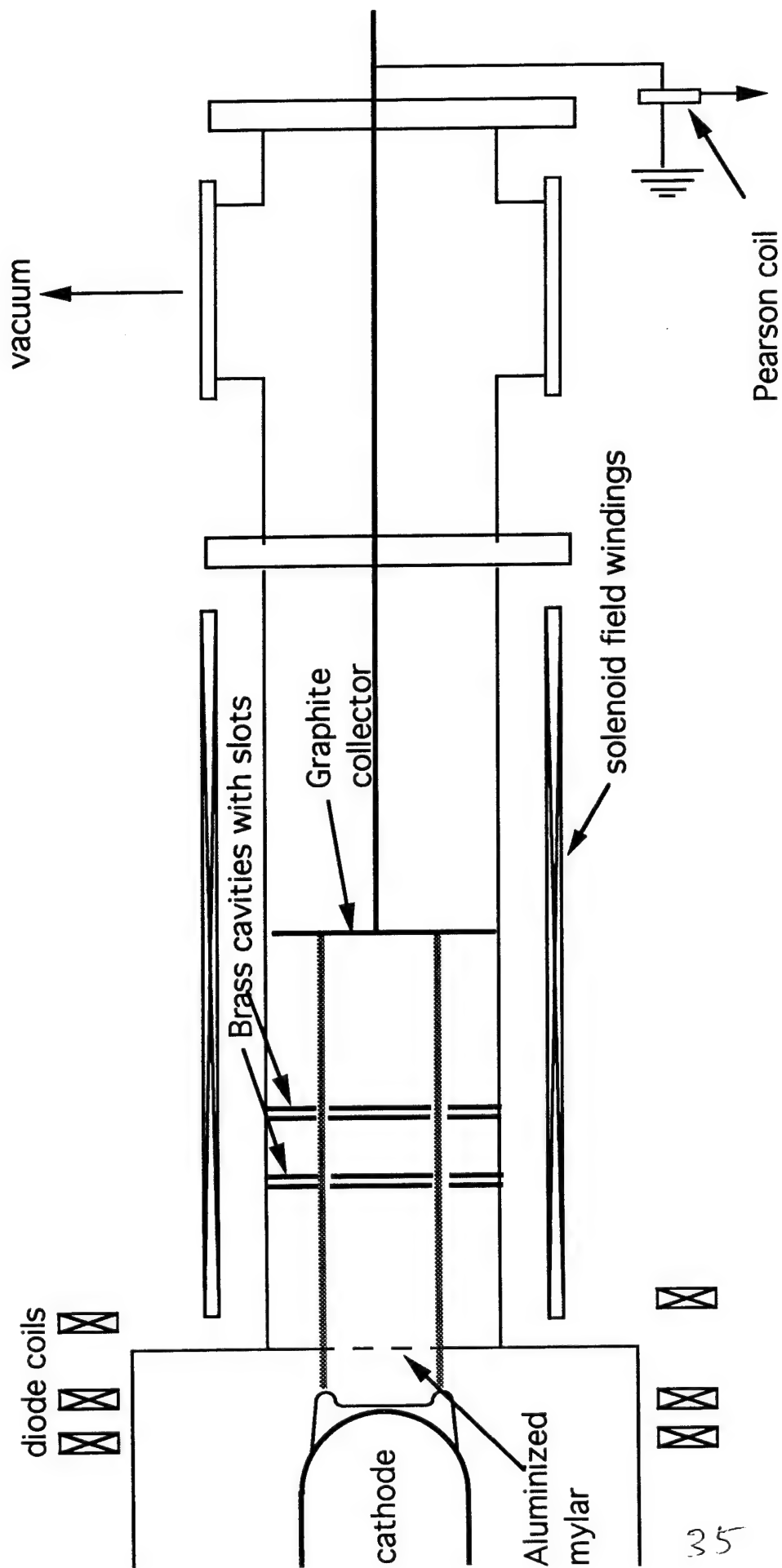
Experimental Parameters:

pulselength: 0.5-0.8 microseconds

Diode current: 1-10 kA

Diode voltage: 0.8 MV

Distance to first cavity (or plate): 40 cm

Distance between first and second cavity: 12 cm

Diode magnetic field: 1 kGauss

Figure 19

Annular Beam Transport Data
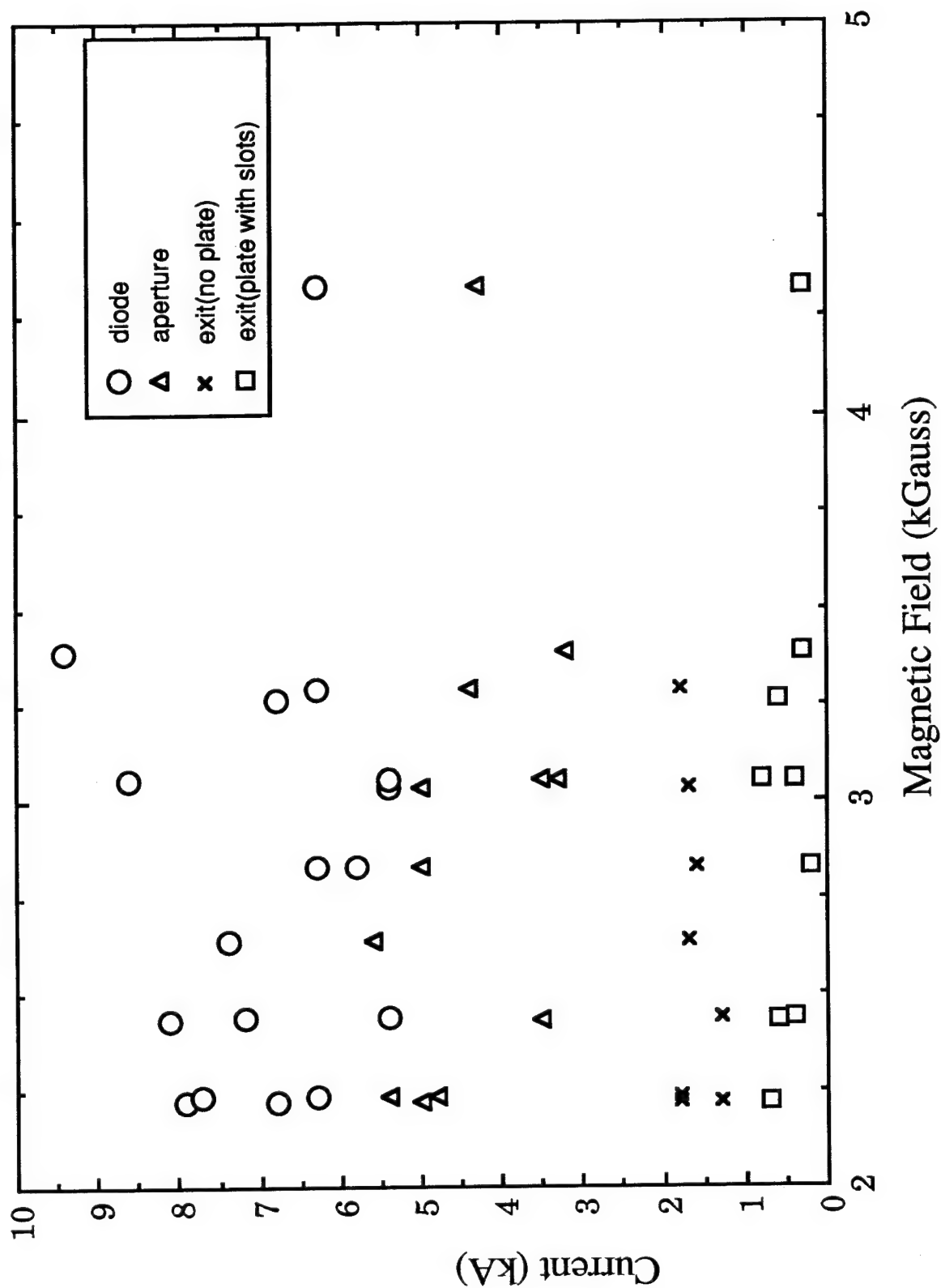
Figure 20

Exit Current vs Magnetic Field
(with and without slotted plate)
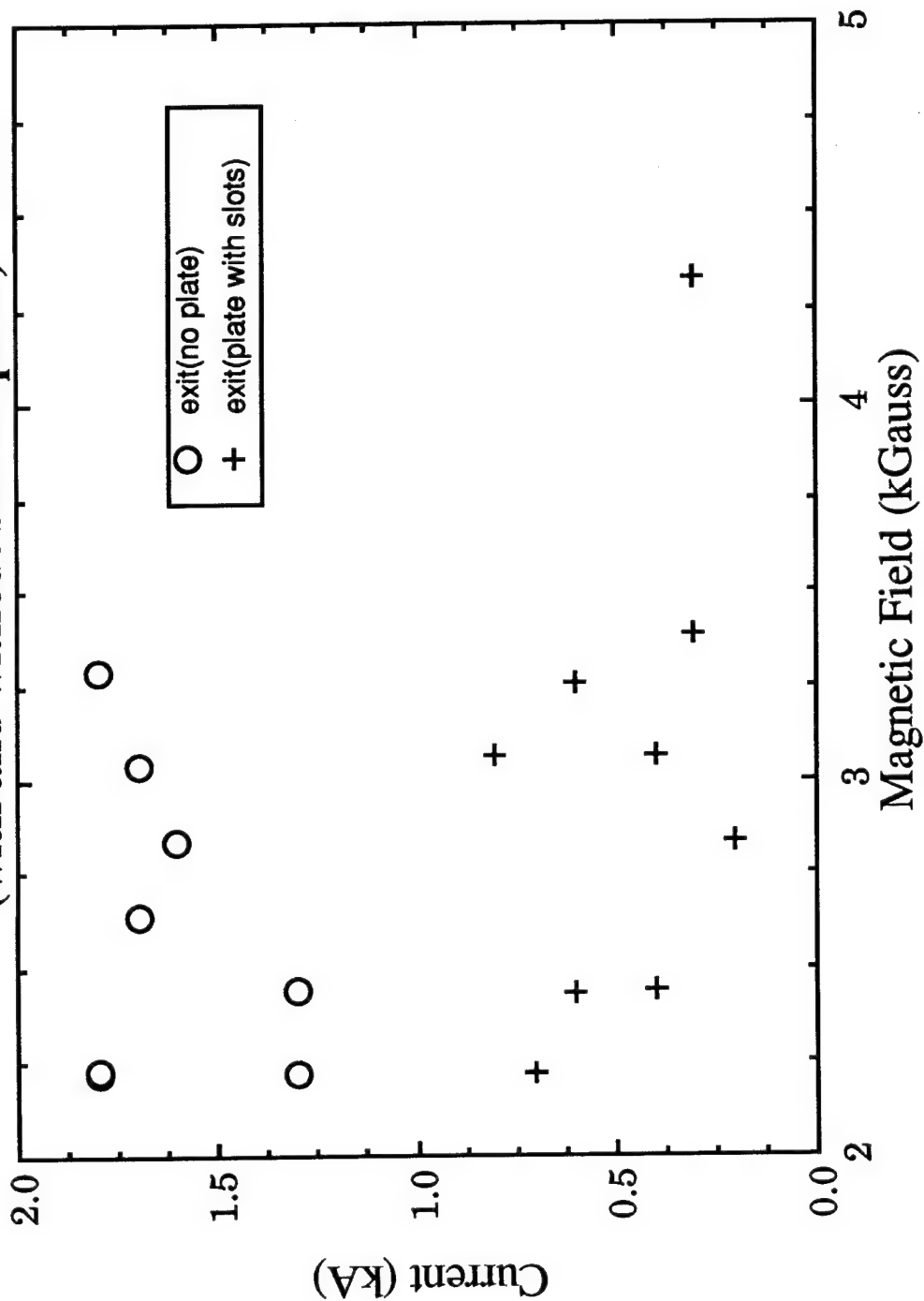
Figure 21

Exit Current Passing Through
Pillbox Cavity vs Magnetic Field
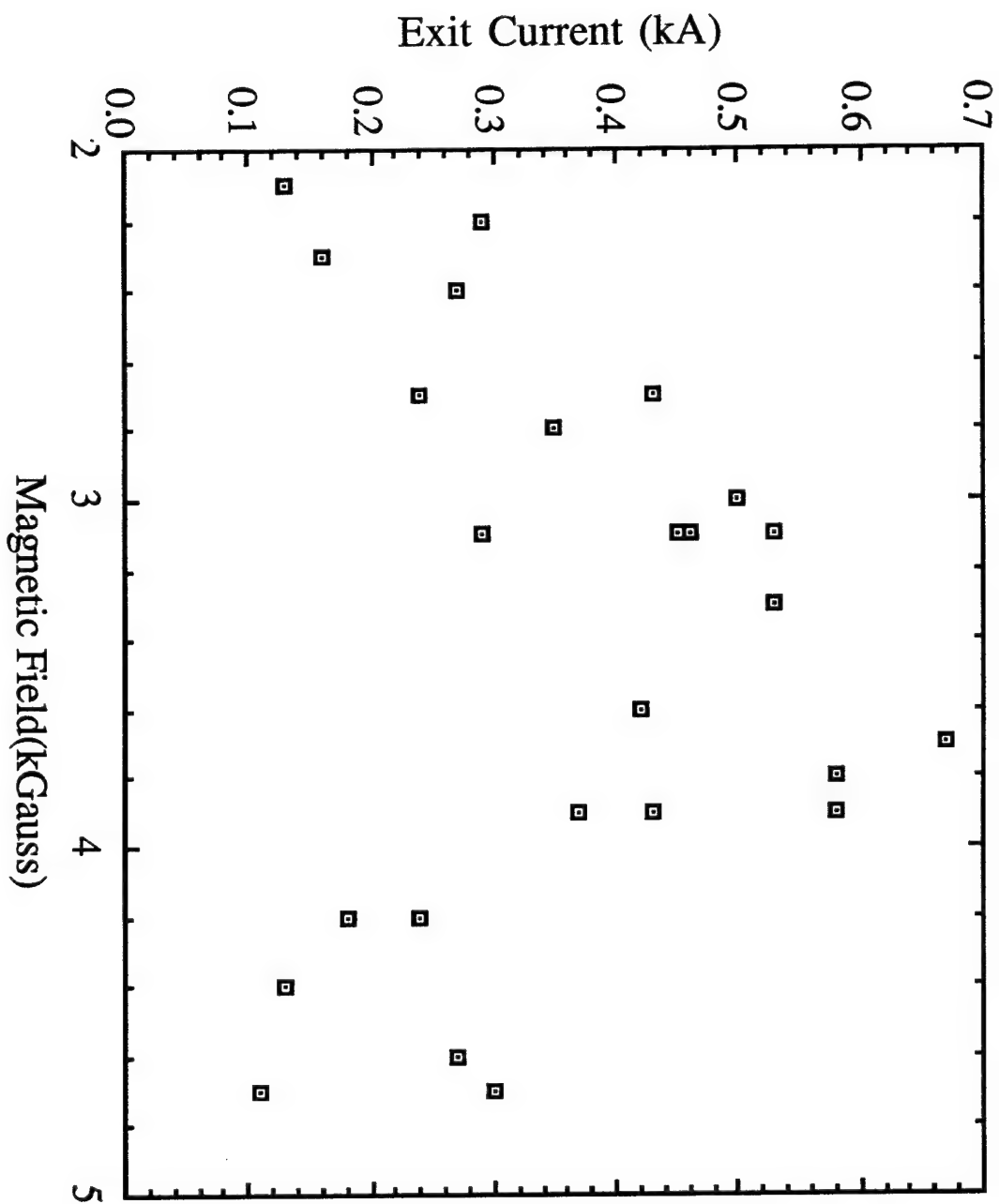
Figure 22

**Transported Exit Current through
Two Pillbox Cavities vs Magnetic Field**

Exit Current (kA)

Magnetic Field (kGauss)
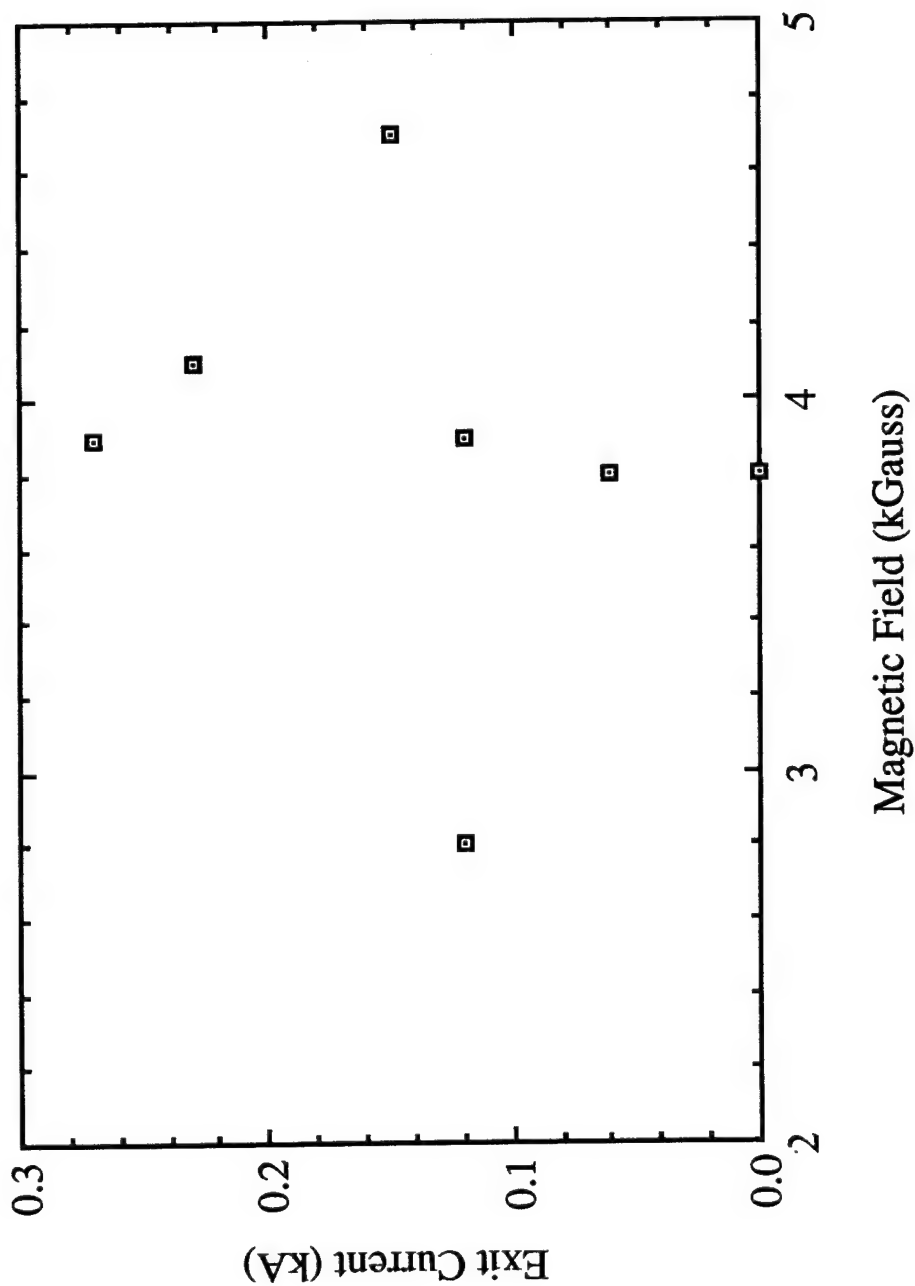
Figure 23

MELBA Shot Number M4317
Magnetic Field 3.7 kGauss

Voltage 200kV/div

Diode current 2kA/div

Anode Aperture Current 2kA/div

Exit current through Pillbox cavity 0.25kA/div

Time (100ns/div)

Figure 24

41

Figure 25

42
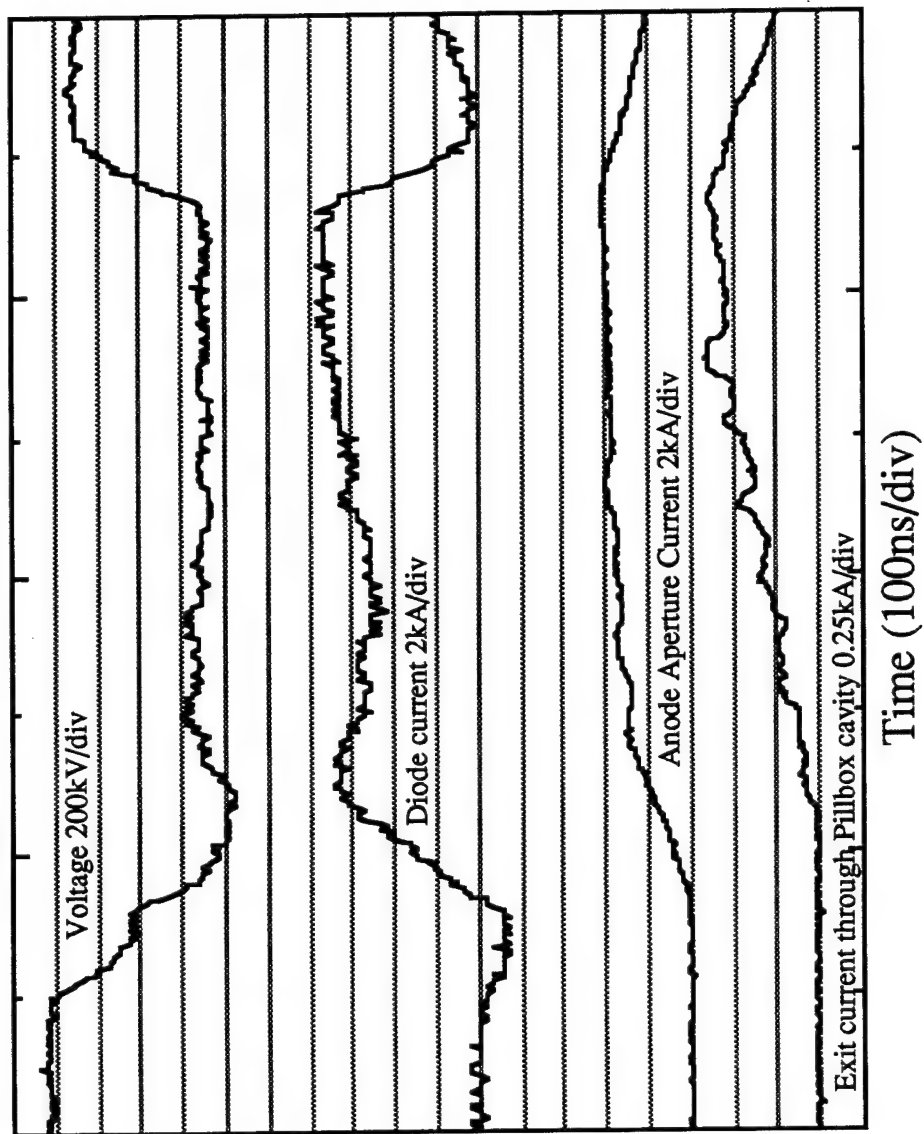
Transported Current vs. Magnetic Field
Rcathode=2.25cm

■ Transported Current (kA)

Transported Current (kA)

Magnetic field (kGauss)

Figure 26

43

Figure 27

diode coils

Beam dump
or diagnostic

primary beam

secondary beam

accelerating
cavities

solenoid

sinusoidal
phase-focusing
coils

high power
microwaves
in

modulating
cavities

cathode

44

Proposal for a Novel Two-Beam Accelerator

Ya. S. Derbenev, Y. Y. Lau, and R. M. Gilgenbach

Intense Energy Beam Interaction Laboratory, Department of Nuclear Engineering,
University of Michigan, Ann Arbor, Michigan 48109-2104

(Received 1 November 1993; revised manuscript received 16 February 1994)

A new configuration is proposed wherein a low-current beam is accelerated to high energies (tens of amps, tens of MeV) by a driver beam of high current and low energy (a few kiloamps, < 1 MeV). The annular driver beam excites the TM_{020} cavity mode of an accelerating structure which transfers its rf power to the on-axis secondary beam. Systematic variation of the driver beam radius provides the secondary beam with phase focusing and adjustable acceleration gradient. A proof-of-principle experiment is suggested.

PACS numbers: 41.75.−i, 29.17.+w

Compact electron and ion accelerators in the 10 MeV range have a wide range of applications, such as treatment of bulk materials, activation analysis, and medical radiation sources. To achieve such an energy at moderate levels of current (tens of amps) requires considerable power, and a natural candidate for a driver is the pulse power system [1,2]. Intense annular electron beams (a few kiloamps, < 1 MeV) extracted from such a system have been modulated efficiently, and the current modulations exhibit a high degree of amplitude and phase stability [3]. These modulated beams have been used to generate ultrahigh power microwaves [4,5] and to accelerate electrons to high energies [6]. They will be used as the driver in the two-beam accelerator to be proposed in this paper.

Various two-beam accelerators have been studied in the past [6–10]. There are significant differences in the present configuration, shown schematically in Fig. 1. The driver beam is an annular beam of radius r_0, carrying an ac current I_d at frequency ω. It passes through an accelerator structure, consisting of N cylindrical pillbox cavities. Each cavity has a radius $b = 5.52c/\omega$ so that ω is also the reson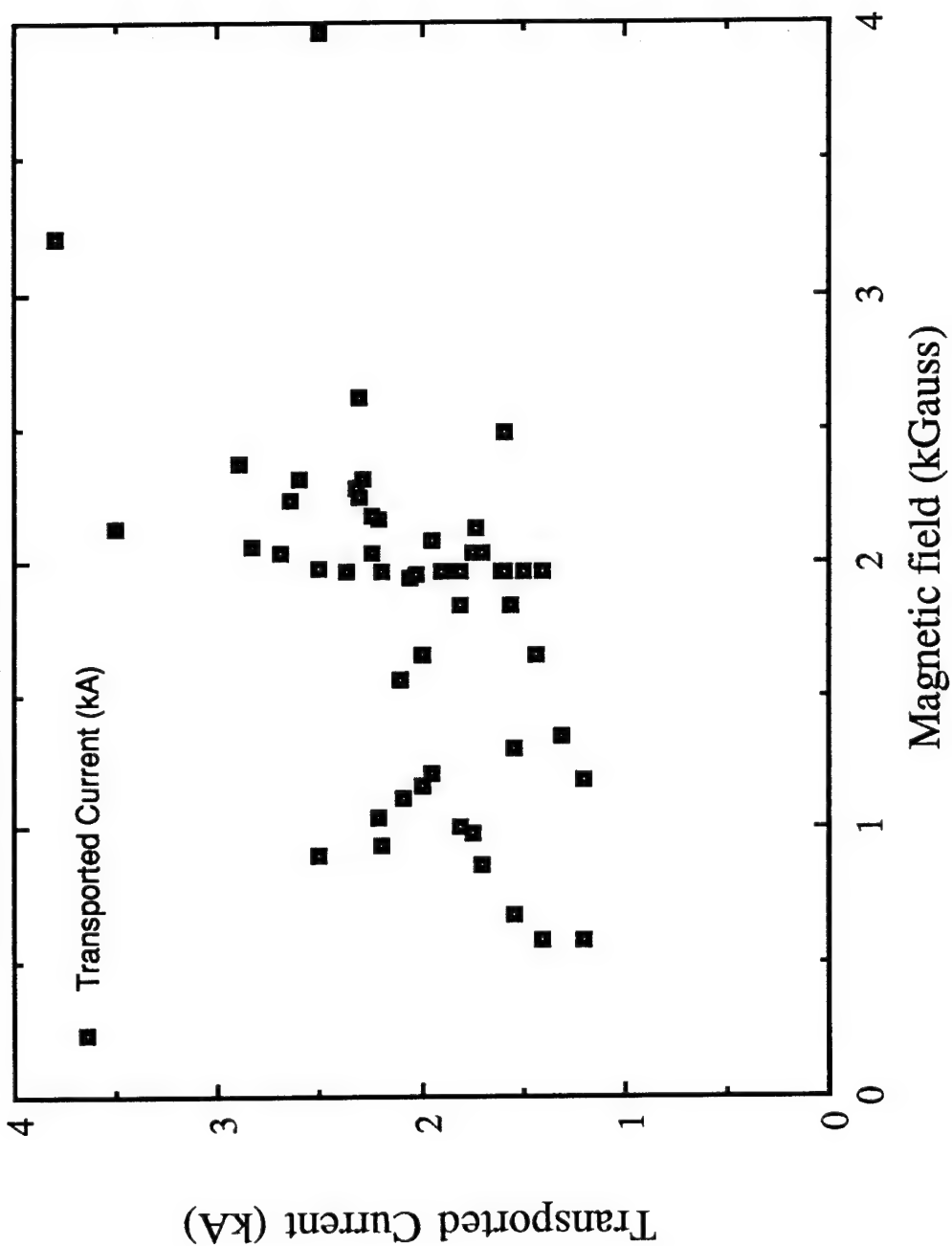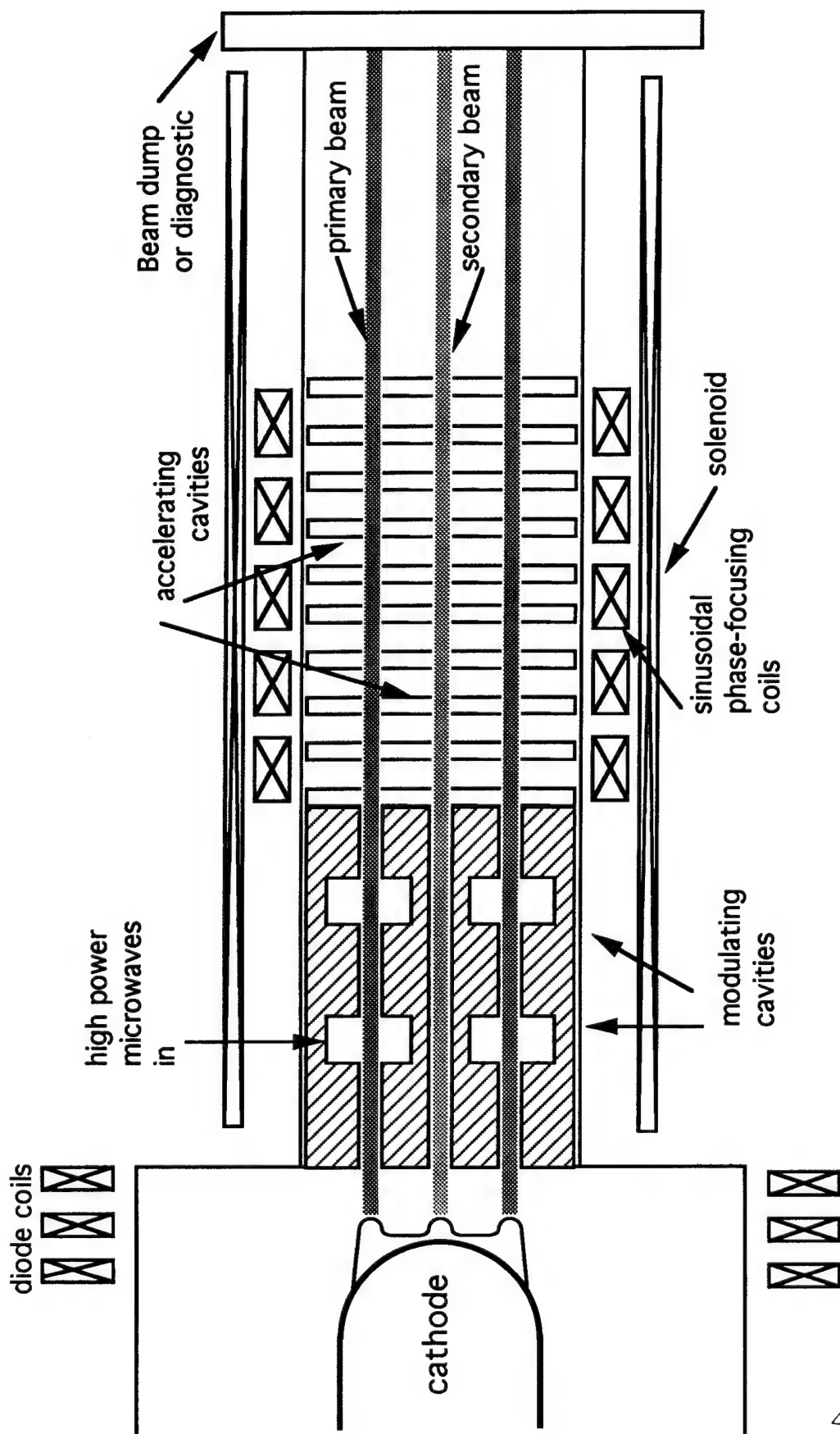ant frequency of the TM_{020} mode of the pillbox cavity (Fig. 1). The secondary beam is an on-axis pencil beam, carrying an ac current I_s ($I_s \ll I_d$), also at frequency ω. Since the rf electric fields of the TM_{020} mode have opposite signs in the outer region and in the inner region, the mode retards the annular driver beam but accelerates the on-axis secondary beam. As we shall see, if the driver beam radius is modulated axially, phase focusing and tunability in the output energy of the secondary beam can be achieved. This is the crucial feature of the present device, not shared by the prior works [6–10].

Thus, without the use of rf plumbing, the present scheme provides the gradual conversion of the primary beam power to the secondary beam over many accelerating gaps. Since the current modulation on the primary beam has been shown to be insensitive to the variations in the diode voltage and diode current [3], the effectiveness in the acceleration of the secondary beam is likewise insensitive to such variations.

To calculate the excitation of the TM_{020} mode by the

primary beam, and the resultant acceleration of the secondary beam by this mode, we assume that the intense space charge on the beam does not alter the rf characteristic of the cavities [4,11,12]. We also assume that the individual pillbox cavities are electromagnetically isolated from each other when the beams are absent [13,14]. Since the cavities are excited mainly by the rf current I_d carried by the primary beam, the TM_{020} mode so excited *always decelerates* the primary beam electrons on the average (by conservation of energy). This is true whether the beam radius r_0 is larger or smaller than a, where $a = 2.405c/\omega$ is the radius of the rf electric field null of the TM_{020} mode [Fig. 2(a)]. The value of the rf electric field at r_0 then gives the deceleration gradient. In terms of the relativistic mass factor (γ_d), the energy loss by this driver beam as it traverses the nth cavity is given by

$$\frac{d\gamma_d}{dn} = -\Lambda\delta^2 \tag{1}$$

in a continuum description. In Eq. (1),

$$\Lambda = 0.066(\omega L/c)Q(I_d/1 \text{ kA}) \tag{2}$$

is the dimensionless parameter that measures the strength of the cavity excitation by the primary beam,

$$\delta = J_0(\omega r_0/c) \approx -1.249(r_0 - a)/a, \tag{3}$$

Q is the quality factor of the TM_{020} mode, L is the cavity length, and J_0 is the Bessel function of the first kind of
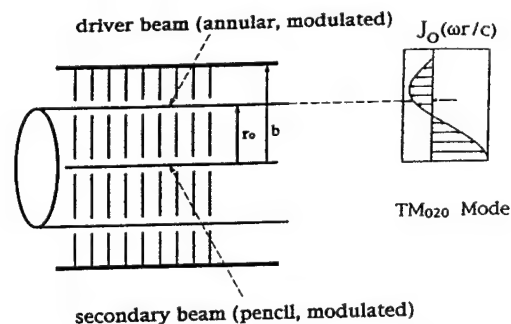

FIG. 1. Schematic drawing of the two-beam accelerator. Also shown is the rf force profile, $J_0(\omega r/c)$, associated with the axial electric field of the TM_{020} cavity mode.
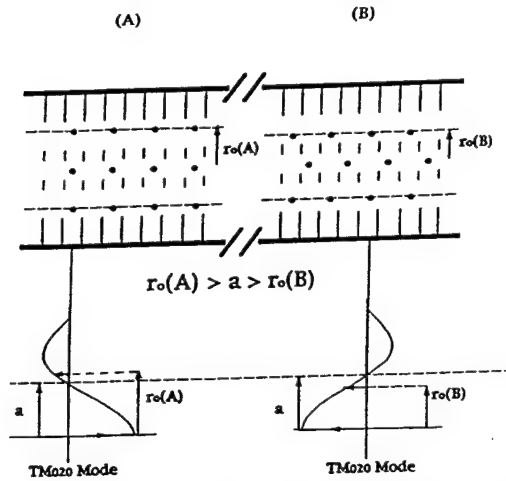
FIG. 2. (a) Position of the primary beam radius r_0 ($r_0 > a$) for secondary beam acceleration when both beams enter the cavity at the same phase. (b) Position of the primary beam radius r_0 ($r_0 < a$) for secondary beam acceleration when both beams enter the cavity at 180° phase apart.

FIG. 3. Evolution of the relativistic mass factors when the driver beam radius r_0 is a constant: (a) the driver beam, (b) the secondary beam. Phase slippage prohibits continual acceleration of the secondary beam.

order zero. In writing the last expression of Eq. (3), we have made the assumption that the annular beam is located in the vicinity of the rf electric field null ($r_0 \approx a$).

If the secondary beam enters the cavity at the same phase as the primary beam, the former will be accelerated if $r_0 > a$, for in this case the rf fields experienced by both beams have opposite polarity [Fig. 2(a)]. Since the rf electric field has a radial dependence of $J_0(\omega r/c)$, it is obvious that $1/|\delta|$ is the "transformer ratio," which is the ratio of the energy gain by the secondary beam to the energy loss by the primary beam, *if both beams enter the cavity at the same phase*. This dependence on the phase is reflected in the following equation which describes the change in the relativistic mass factor (γ_s) of the secondary beam as it traverses the nth cavity:

$$\frac{d\gamma_s}{dn} = -\Lambda\delta\cos(\theta_s - \theta_d), \tag{4}$$

where θ_s is the phase of the secondary beam bunch and θ_d is the phase of the primary beam bunch when they enter the nth cavity. Equation (4) is readily obtained from Eq. (1) by noting the transformer ratio $1/\delta$ and the phase difference mentioned above. Equations (3) and (4) indeed show that γ_s increases if $r_0 > a$ and if $\theta_d = \theta_s$.

The secondary beam cannot be accelerated indefinitely because of the increase in the phase slippage between θ_d and θ_s downstream. This phase slippage occurs as the primary beam is decelerated and the secondary beam is accelerated. Its rate of increase is governed by

$$\frac{d(\theta_s - \theta_d)}{dn} = \frac{\omega L}{c}\left[\frac{1}{\beta_s} - \frac{1}{\beta_d}\right]$$
$$= \frac{\omega L}{c}[(1 - 1/\gamma_s^2)^{-1/2} - (1 - 1/\gamma_d^2)^{-1/2}]. \tag{5}$$
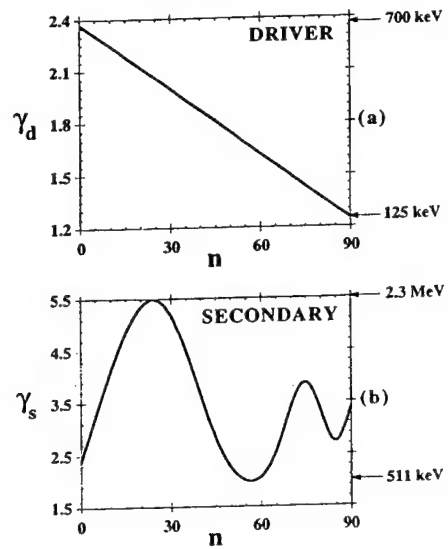
The effect on the secondary beam by this phase slippage is illustrated in Fig. 3, which is obtained by numerically solving the system of three equations [(1), (4), (5)] in three unknowns: γ_d, γ_s, and $\theta_s - \theta_d$. The initial conditions for these three unknowns are taken to be $\theta_s - \theta_d = 0$ and $\gamma_d = \gamma_s = 2.37$, corresponding to an initial energy of 700 keV for both beams. The other parameters are $\omega/2\pi = 3.65$ GHz, $b = 7.221$ cm, $L = 1$ cm, $a = 3.146$ cm, $r_0 = 3.322$ cm, $Q = 100$, and $I_d = 0.5$ kA. Since we have taken $L = 1$ cm, the cavity number n is also the axial distance (z) in cm.

Figure 3(a) shows that γ_d decreases from the initial value of 2.37 to 1.24 at $n = 90$; i.e., the primary beam's energy steadily decreases from 700 to 125 keV after propagating 90 cm. The secondary beam's energy [Fig. 3(b)] increases initially, reaching a maximum value of 2.3 MeV after 24 cm, and then decreases due to the phase slippage until $n = 56$, and oscillates further downstream as the phase slippage continues.

The phase slippage may be corrected by adjusting the primary beam's radius r_0. Consider, for example, the worst case of phase slippage where the primary beam and the secondary beam arrive at a cavity 180° out of phase, as shown in Fig. 2(b). If the primary beam's radius r_0 is *less* than a, it generates an rf electric field which would retard *both* beams during the time when the *primary* beam occupies the cavity. However, when the charge bunch of the primary beam resides in the cavity, there are few particles in the secondary beam residing in the same cavity because both beams arrive at the cavity 180° out of phase. By the time the charge bunch of the primary beam is about to leave the cavity, the rf electric field is about to change sign, at which time the charge bunch of the secondary beam is about to enter the cavity, whose rf electric field then begins to accelerate the entering bunch

46

on the secondary beam. Thus, the phase slippage problem can be corrected by a simple cure: At the locations where the bunches of both beams enter the cavity with the same phase, place r_0 outside a. When the bunches of both beams arrive at the cavity 180° out of phase, place r_0 inside a.

Mathematically, it is easy to see from Eqs. (3) and (4) that γ_s is a monotonically increasing function of n if r_0 is tapered in such a way that $(r_0 - a)\cos(\theta_s - \theta_d) \geq 0$.

The above idea of phase slippage correction has been tested for the example shown in Figs. 3(a) and 3(b). From that figure, the phase slippage occurs with a period of the order of 75 cm. Thus, we correct the primary beam radius r_0 according to

$$r_0(\text{cm}) = 3.146 + (3.322 - 3.146)\cos(2\pi n/75). \quad (6)$$

Including only this modification, and keeping all other parameters the same, we obtain Fig. 4. In Fig. 4, we see that the primary beam's energy monotonically decreases from 700 to 400 keV over 90 cm, whereas the secondary beam's energy increases monotonically from 700 keV to a maximum of 4.2 MeV over the same distance, in sharp contrast to Fig. 3(b). The loss of 300 keV in the primary beam and the gain of 3.5 MeV in the secondary beam implies an effective transformer ratio of about (3.5 MeV)/(300 keV)=11.7.

In Fig. 4, the zero slopes in γ_s and in γ_d occur at the axial positions (n) at which the driver beam radius r_0 coincides with the field-null position a. The slight dip in γ_s at $n = 90$ only means that the primary beam's radius r_0 needs further adjustment there. If we write $r_0 = a + \Delta\cos(\psi)$, where Δ is the amplitude and ψ is the phase of the modulation in r_0, the general phase focusing condition reads $d\psi/dn = d(\theta_s - \theta_d)/dn$. This condition is applicable when the two beams have different velocities. In fact, one might argue that this technique of radius modulation provides both beams with self-focusing in phase, similar to the self-focusing in synchrotrons [15].

The modulation in the annular beam radius may be readily achieved by a proper adjustment of the external solenoidal magnetic field which is often used for beam focusing and beam transport [3–6,14]. Since the rate of change of energy depends on the annular beam radius r_0 [cf. Eqs. (1) and (3)], the output energy of the accelerated beam may also be controlled by the same external magnetic field coils.

The above ideas may be tested in a proof-of-principle experiment with parameters similar to those used to produce Fig. 4. The primary beam may be obtained, for example, from the Michigan Electron Long-Beam Accelerator (MELBA) [16], which operates with diode parameters of 700 keV, current up to 10 kA, and flattop pulse length up to 1 μs. This primary beam may be modulated using the proven techniques by Friedman et al. [3,4,6]. Note that the average acceleration gradient of 40 kV/cm and the peak acceleration gradient of about 80 kV/cm implied by Fig. 4 are well within the rf break-
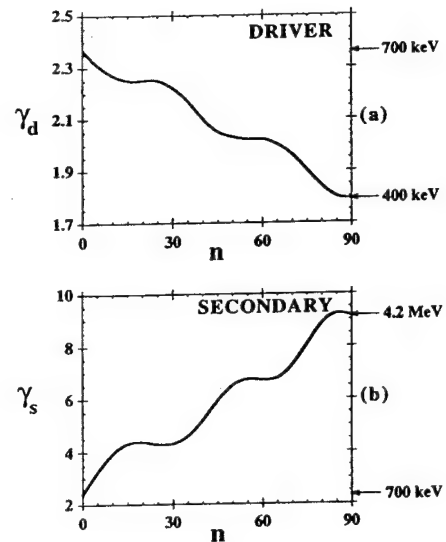

FIG. 4. Evolution of the relativistic mass factors when the driver beam radius r_0 is modulated to compensate phase slippage: (a) the driver beam, (b) the secondary beam.

down limit. If we assume an acceleration efficiency of 25%, a secondary beam of more than 10 A of current may be accelerated to 4 MeV in less than a meter in this proof-of-principle experiment.

There are many issues which may affect the eventual usefulness of the two-beam accelerator concept outlined above. Chief among them is the modification of the rf characteristic that always accompanies an intense driver beam, which includes a detuning of the structure frequency and a modification of the gap transit-time factor [4,11,12,17]. Also of concern is the beam breakup instability (BBU) on the driver beam [10,13,14,17]. However, we have recently found that BBU in an annular beam may be far less serious than a pencil beam [18], and BBU can be controlled by many well-known techniques [19]. The degree of coupling among neighboring cavities, especially in the presence of an intense beam, remains to be studied [20]. Although the driver beam's radius is a crucial factor, the effects of the beam's finite thickness are far less important, according to our preliminary studies. We have also examined the effects of the transverse wake [21] and of the longitudinal instabilities [22] and found that they are not serious, at least for the parameters used in the above numerical example, assuming a solenoidal field of 10 kG in the accelerating structure.

In summary, we propose a novel scheme which has the potential of converting many existing pulse power systems into compact rf accelerators that are suitable for industrial and medical applications. The driver beam is a modulated intense relativistic electron beam of annular shape and low energy (< 1 MeV). The secondary beam is an on-axis pencil beam. The secondary beam may reach an energy up to 10 MeV in 1 to 2 m. Phase focusing and energy tunability of the accelerated beam may be provided by an external magnetic field, which controls the radius of the primary beam. While we have in this paper con-

centrated only on electron acceleration in the 10 MeV range, it is intriguing to speculate on the potential of using this technique (a) to accelerate ions to tens of MeV, and (b) to accelerate electrons to ultrahigh energy using superconducting cavities [cf. Eq. (2)] and higher energy driver beams.

[1] J. C. Martin (unpublished); see also the survey by J. A. Nation, Part. Accel. **10**, 1 (1979).

[2] S. Humphries, *Charged Particle Beams* (Wiley, New York, 1990); R. C. Davidson, *Physics of Nonneutral Plasmas* (Addison-Wesley, Redwood City, CA, 1990); R. B. Miller, *Intense Charged Particle Beams* (Plenum, New York, 1982).

[3] M. Friedman and V. Serlin, Phys. Rev. Lett. **55**, 2860 (1985); M. Friedman *et al.*, J. Appl. Phys. **64**, 3353 (1988); J. Krall and Y. Y. Lau, Appl. Phys. Lett. **52**, 431 (1988).

[4] M. Friedman *et al.*, Rev. Sci. Instrum. **61**, 171 (1990); Y. Y. Lau *et al.*, IEEE Trans. Plasma Sci. **18**, 553 (1990).

[5] See, e.g., Proc. SPIE Int. Soc. Opt. Eng. **1407** (1991); **1629** (1992); **1872** (1993) (edited by H. E. Brandt).

[6] M. Friedman *et al.*, Phys. Rev. Lett. **63**, 2468 (1989).

[7] M. A. Allen *et al.*, Phys. Rev. Lett. **63**, 2472 (1989); A. M. Sessler and S. S. Yu, *ibid.* **58**, 2439 (1987).

[8] G. Voss and T. Weiland, DESY Report No. M82-10, 1982 (unpublished); DESY Report No. M82-079, 1982 (unpublished).

[9] W. Gai *et al.*, Phys. Rev. Lett. **61**, 2765 (1988); H. Figueroa *et al.*, *ibid.* **60**, 2144 (1988); J. B. Rosenzweig *et al.*, Phys. Fluids B **2**, 1376 (1990).

[10] A. M. Sessler *et al.*, Part. Accel. **31**, 1277 (1990); Nucl. Instrum. Methods Phys. Res., Sect. A **306**, 592 (1991); D. B. Hopkins *et al.*, Nucl. Instrum. Methods Phys. Res. **228**, 15 (1984); D. H. Whittum *et al.*, Phys. Rev. A **43**, 294 (1991); also in "Advanced Accelerator Concepts," edited by J. Wurtele, AIP Conf. Proc. No. 279 (AIP, New York, to be published).

[11] P. B. Wilson, in *Physics of High Energy Particle Accelerators*, edited by R. A. Carrigan *et al.*, AIP Conf. Proc. No. 87 (AIP, New York, 1982), p. 452.

[12] D. G. Colombant and Y. Y. Lau, Phys. Rev. Lett. **64**, 2320 (1990).

[13] This is similar to the cumulative beam breakup instability, suggested by W. K. H. Panofsky and M. Bander, Rev. Sci. Instrum. **39**, 206 (1968).

[14] See, e.g., P. R. Menge, R. M. Gilgenbach, and Y. Y. Lau, Phys. Rev. Lett. **69**, 2372 (1992); Y. Y. Lau, *ibid.* **63**, 1141 (1989), and references therein.

[15] See, e.g., E. D. Courant, in *Physics of High Energy Particle Accelerators* (Ref. [11]), p. 2.

[16] R. M. Gilgenbach *et al.*, in *Digest of Fifth IEEE Pulse Power Conference* (IEEE, New York, 1985), p. 126.

[17] P. Menge, Ph.D thesis, University of Michigan, Ann Arbor, 1993.

[18] Y. Y. Lau and J. W. Luginsland, J. Appl. Phys. **74**, 5877 (1993). In the line above Eq. (7) of this paper, the factor [$I/(1$ kA)] should read [$I/(17$ kA)].

[19] In the absence of other stabilizing mechanisms such as stagger tune and betatron frequency spread, we estimate that a solenoidal magnetic field of 10 kG and a dipole mode Q of 100 would limit the *worst* BBU growth to $1.8e$-fold (in amplitude) for a 500 ns, 0.5 kA beam in a 90 cm accelerator structure, as in the numerical example.

[20] There are several ways to reduce the coupling among neighboring cavities. The inductive coupling at the annular hole, through which the driver beam passes, may be canceled by the capacitive coupling at the center hole, and if necessary, by introducing additional holes near the rf electric field maximum (so as to increase the capacitive coupling) that is close to the outer wall of the cavity (Fig. 1). Alternatively, conducting wires may be inserted radially across the annular gap to reduce the inductive coupling. Multiple pencil beams may also be used as the driver. These pencil beams pass through holes that are distributed annularly. In the event that the neighboring cavities are not completely isolated electromagnetically, a traveling wave formulation would be required; but the radius modulation that is proposed in this paper still provides an external control to ensure phase focusing.

[21] We estimate that a nominal value of solenoidal field $B_0 = 10$ kG would render the effects of the transverse wake field on the driver beam unimportant. Specifically, under the condition $\Omega \gg \omega/\gamma_d(1+\beta_d)$, where Ω is the nonrelativistic cyclotron frequency associated with B_0 and the other symbols are the same as in Eq. (5), the electron motion is adiabatic along the composite (dc+rf) magnetic field line. The maximum angular displacement, from the mean, is estimated to be $l_\theta = 0.52(c/\omega)(E_a/cB_0)\beta_d/(1-\beta_d)$ where E_a is the maximum accelerating electric field experienced by the secondary beam. The maximum radial displacement is $l_r = l_\theta \lambda_L/\lambda_m$, where $\lambda_L = 2\pi\beta_d\gamma_d c/\Omega$ and λ_m is the axial wavelength associated with the modulation in the driver beam radius. For the parameters used in the numerical example, $l_\theta \leq 0.2$ cm, and $l_r \leq 0.0058$ cm. The spread in momentum, dp, in the driver beam may introduce a variation in its annular beam radius, dr_0. It is estimated that $dr_0 \leq [2(\lambda_L^2/\lambda_m^2)\Delta + 0.083\lambda_L E_a/cB_0]dp/p$, where Δ is the amplitude of the modulation in the driver beam radius. Using the parameters in the numerical example, we find $dr_0 < 0.0061$ cm if $dp/p < 1$. Thus, the effectiveness of radius modulation is not affected by momentum spread.

[22] We conjecture that the longitudinal (Robinson-like) instability probably is not important for the present scheme, at least in the proposed proof-of-principle experiment. Unlike a circular accelerator, the present scheme is single pass. Its acceleration length is quite short; its length is only slightly over one wavelength in the radius modulation. Moreover, the drive frequency may be adjusted to be on the "right side" of the structure frequency to avoid the Robinson-like instability.

48

A Novel Two-Beam Accelerator (Twobetron)

Y. Y. Lau, Ya. S. Derbenev, R. M. Gilgenbach,
J. W. Luginsland, J. M. Hochman, and M. T. Walter

Intense Energy Beam Interaction Laboratory
Department of Nuclear Engineering
University of Michigan
Ann Arbor, Michigan 48109-2104

Abstract. A new configuration is analyzed wherein a low current beam is accelerated to high energies (10's of amps, 10's of MeV) by a driver beam of high current and low energy (a few kiloamps, < 1 MeV). The annular driver beam excites the TM_{020} cavity mode of an accelerating structure which transfers its rf power to the on-axis secondary beam. Systematic variation of the driver beam radius provides the secondary beam with phase focusing and adjustable acceleration gradient. A proof-of-principle experiment is suggested. Various issues, such as the scaling laws, transverse and longitudinal instabilities, rf coupling among cavities, etc., are examined.

INTRODUCTION

Two-beam accelerators have been studied extensively in the high energy physics community [1]. This paper concentrates on the 10 MeV range. Compact electron and ion accelerators in this energy range have a wide range of applications, such as treatment of bulk materials, activation analysis, and medical radiation sources. To achieve such an energy at moderate levels of current (tens of amps) requires considerable power, and a natural candidate for a driver is the pulse power system. Intense annular electron beams (multi-kiloamps, < 1 MeV) extracted from such a system have been modulated efficiently, and the current modulations exhibit a high degree of amplitude and phase stability [2]. Their successful applications [3] in ultra-high power microwave generation and in particle acceleration have motivated us to use them as drivers in a novel two-beam accelerator [4], termed "twobetron" hereafter.

The twobetron is shown schematically in Fig. 1. The driver beam is an annular beam of radius r_0, carrying an AC current I_d at frequency ω. It passes through an accelerator structure, consisting of N cylindrical pillbox cavities. Each cavity has a radius $b = 5.52\ c/\omega$ so that ω is also the resonant frequency of the TM_{020} mode of the pillbox cavity [Fig. 1]. The secondary beam is an on-axis pencil beam, carrying an AC current I_s ($I_s \ll I_d$), also at frequency ω. Since the rf electric fields of the TM_{020} mode have opposite signs in the outer region and in the inner region, the mode retards the annular driver beam but accelerates the on-axis secondary beam. If the driver beam radius is modulated axially, phase focusing and tunability in the output energy of the secondary beam can be

achieved. This phase focusing technique thus also offers the possibility of using much lower driver beam voltage (e.g., 100 keV), a distinct advantage in many applications.
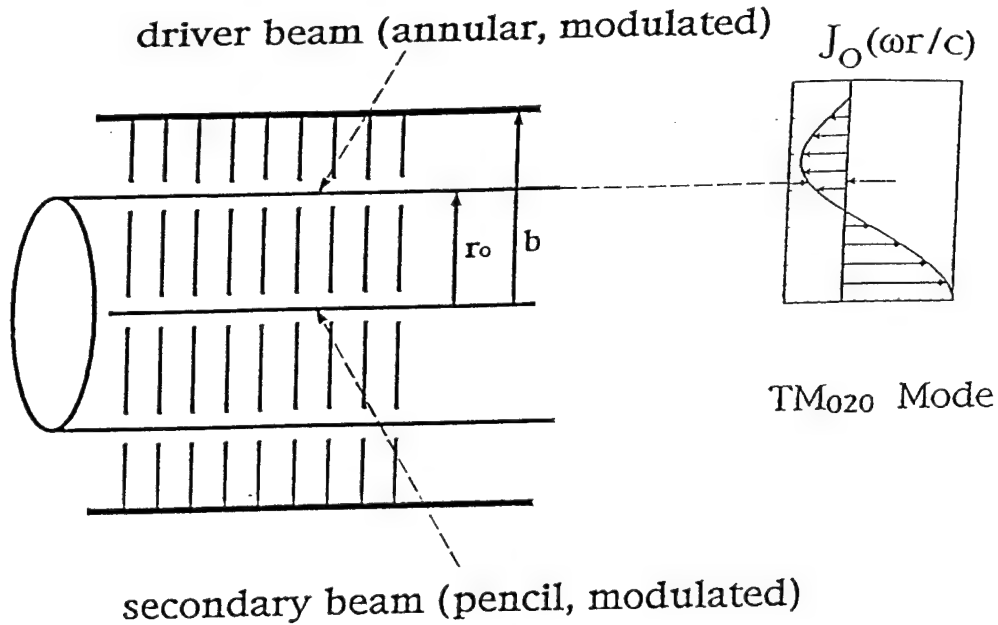
Figure 1. Schematic drawing of the two-beam accelerator. Also shown is the rf force profile, $J_0(\omega r/c)$, associated with the axial electric field of the TM$_{020}$ cavity mode.

ACCELERATION MECHANISM

To calculate the excitation of the TM$_{020}$ mode by the primary beam, and the resultant acceleration of the secondary beam by this mode, we assume that the intense space charge on the beam does not alter the rf characteristic of the cavities. We also assume, for the time being, that the individual pillbox cavities are electromagnetically isolated from each other when the beams are absent. Since the cavities are excited mainly by the rf current I_d carried by the primary beam, the TM$_{020}$ mode so excited <u>always decelerates</u> the primary beam electrons on the average (by conservation of energy). This is true whether the beam radius r_0 is larger or smaller than a, where a = 2.405 c/ω is the radius of the rf electric field null of the TM$_{020}$ mode [Fig. 2a]. The value of the rf electric field at r_0 then gives the deceleration gradient. In terms of the relativistic mass factor (γ_d), the energy loss by this driver beam as it traverses the n-th cavity is given by

$$\frac{d\gamma_d}{dn} = -\Lambda\delta^2, \tag{1}$$

in a continuum description. In Eq. (1),

$$\Lambda = 0.066(\omega L / c)Q(I_d / 1kA) \tag{2}$$

is the dimensionless parameter that measures the strength of the cavity excitation by the primary beam,

$$\delta = J_0(\omega r_0 / c) \approx -1.249(r_0 - a) / a, \tag{3}$$

Q is the quality factor of the TM_{020} mode, L is the cavity length, J_0 is the Bessel function of the first kind of order zero. In writing the last expression of Eq. (3), we have made the assumption that the annular beam is located at the vicinity of the rf electric field-null ($r_0 \approx a$).
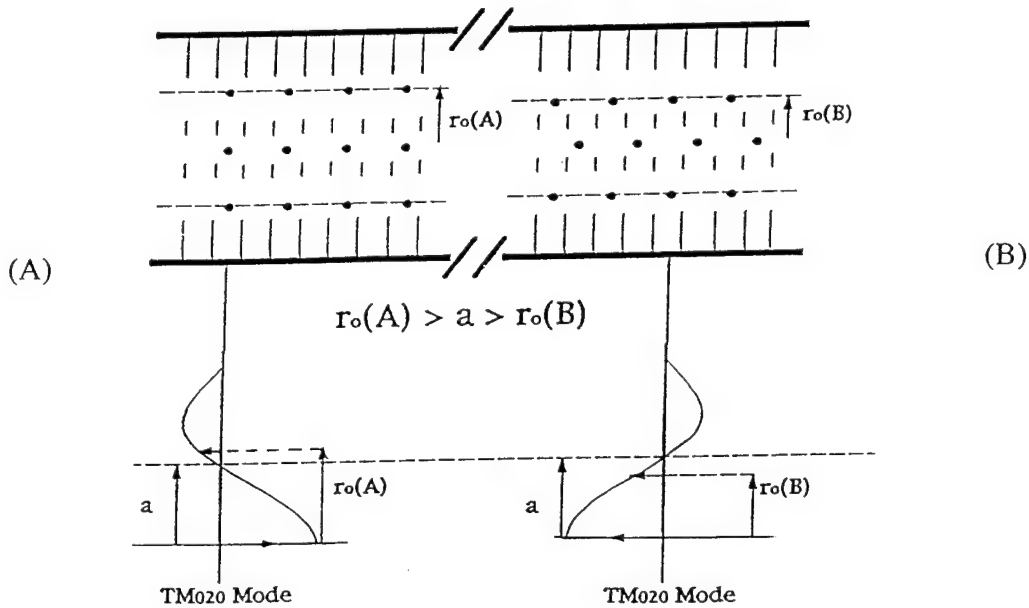

Figure 2.
(a) Left. Position of the primary beam radius r_0 ($r_0 > a$) for secondary beam acceleration when both beams enter the cavity at the same phase.
(b) Right. Position of the primary beam radius r_0 ($r_0 < a$) for secondary beam acceleration when both beams enter the cavity at 180° apart phase.

If the secondary beam enters the cavity at the same phase as the primary beam, the former will be accelerated if $r_0 > a$, for in this case the rf fields experienced by both beams have opposite polarity [Fig. 2a]. Since the rf electric field has a radial dependence of $J_0(\omega r / c)$, it is obvious that $1/|\delta|$ is the "transformer ratio", which is the ratio of the energy gain by the secondary beam to the energy loss by the primary beam, if both beams enter the cavity at the same phase. This dependence on the phase is reflected in the following equation which describes the change in the relativistic mass factor (γ_s) of the secondary beam as it traverses the n-th cavity:

$$\frac{d\gamma_s}{dn} = -\Lambda\delta \cdot \cos(\theta_s - \theta_d), \tag{4}$$

where θ_s is the phase of the secondary beam bunch and θ_d is the phase of the primary beam bunch when they enter the n-th cavity. Equation (4) is readily obtained from Eq. (1) by noting the transformer ratio $1/\delta$ and the phase difference mentioned above. Equations (3) and (4) indeed show that γ_s increases if $r_0 > a$ and if $\theta_d = \theta_s$.

The secondary beam cannot be accelerated indefinitely because of the increase in the phase slippage between θ_d and θ_s downstream. This phase slippage occurs as the primary beam is decelerated and the secondary beam is accelerated. Its rate of increase is governed by

$$\frac{d(\theta_s - \theta_d)}{dn} = \frac{\omega L}{c}\left(\frac{1}{\beta_s} - \frac{1}{\beta_d}\right) = \frac{\omega L}{c}\left[\frac{1}{\sqrt{1 - 1/\gamma_s^2}} - \frac{1}{\sqrt{1 - 1/\gamma_d^2}}\right]. \tag{5}$$

The effect on the secondary beam by this phase slippage is illustrated in Fig. 3, which is obtained by numerically solving the system of three equations [(1), (4), (5)] in three unknowns: γ_d, γ_s, $\theta_s - \theta_d$. The initial conditions for these three unknowns are taken to be: $\theta_s - \theta_d = 0$, $\gamma_d = \gamma_s = 2.37$, corresponding to an initial energy of 700 keV for both beams. The other parameters are : $\omega/2\pi = 3.65$ GHz, b = 7.221 cm, L = 1 cm, a = 3.146 cm, $r_0 = 3.322$ cm, Q = 100, $I_d = 0.5$ kA. Since we have taken L = 1 cm, the cavity number n is also the axial distance (z) in cm.

Figure 3a shows that γ_d decreases from the initial value of 2.37 to 1.24 at n=90, i.e., the primary beam's energy steadily decreases from 700 keV to 125 keV after propagating 90 cm. The secondary beam's energy [Fig. 3b] increases initially, reaching a maximum value of 2.3 MeV after 24 cm, and then decreases

4

52

due to the phase slippage until n= 56, and oscillates further downstream as the phase slippage continues.
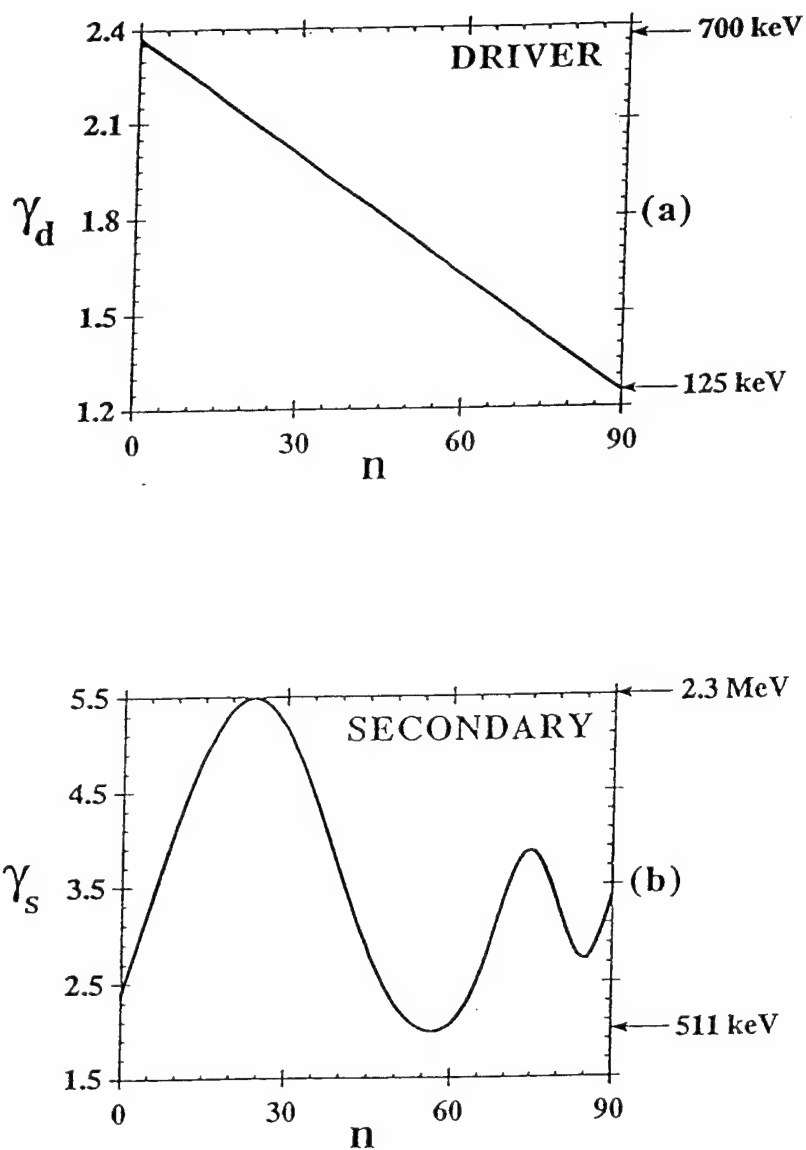

Figure 3. Evolution of the relativistic mass factors when the driver beam radius r_0 is a constant: (a) the driver beam, (b) the secondary beam. Phase slippage prohibits continual acceleration of the secondary beam.

The phase slippage may be corrected [4] by adjusting the primary beam's radius r_0. Consider, for example, the worst case of phase slippage where the primary beam and the secondary beam arrive at a cavity 180° out of phase, as shown in Fig. 2b. If the primary beam's radius r_0 is less than a, it generates an rf electric field which would retard both beams during the time when the primary beam occupies the cavity. However, when the charge bunch of the primary beam resides in the cavity, there are few particles in the secondary beam residing in the same cavity because both beams arrive at the cavity 180° out of phase. By the time the charge bunch of the primary beam is about to leave the cavity, the rf electric field is about to change sign, at which time the charge bunch of the secondary beam is about to enter the cavity, whose rf electric field then begins to accelerate the entering bunch on the secondary beam. Thus, the phase slippage problem can be corrected by a simple cure: At the locations where the bunches of both beams enter the cavity with the same phase, place r_0 outside a. When the bunches of both beams arrive at the cavity 180° out of phase, place r_0 inside a.

Mathematically, it is easy to see from Eqs. (3) and (4) that γ_s is a monotonically increasing function of n if r_0 is tapered in such a way that $(r_0 - a)\cos(\theta_s - \theta_d) \geq 0$. Thus, if we write the primary beam radius r_0 as

$$r_0 - a = \Delta\cos(\psi), \tag{6}$$

where Δ is the amplitude and ψ is the phase of the modulation in r_0, the general phase focusing condition reads

$$d\psi / dn = d(\theta_s - \theta_d) / dn. \tag{7}$$

Including this modification, with $\Delta = 3.322$ cm - 3.146 cm = 0.176 cm, and keeping all other parameters the same as in Fig. 3, we obtain Fig. 4. In Fig. 4, we see that the primary beam's energy monotonically decreases from 700 keV to 415 keV over 90 cm, whereas the secondary beam's energy increases monotonically from 700 keV to a maximum of 4.8 MeV over the same distance, in sharp contrast to Fig. 3b. The loss of 285 keV in the primary beam and the gain of 4.1 MeV in the secondary beam implies an effective transformer ratio of about 4.1 MeV/285 keV =14.4.

The modulation in the annular beam radius may be readily achieved by a proper adjustment of the external solenoidal magnetic field which is often used for beam focusing and beam transport. Since the rate of change of energy depends on the annular beam radius r_0 [cf. Eqs. (1), (3)], the output energy of the accelerated beam may also be controlled by the same external magnetic field coils.

The above ideas may be tested in a proof-of-principle experiment with parameters similar to those used to produce Fig. 4. The primary beam may be

obtained, for example, from the Michigan Electron Long-Beam Accelerator (MELBA [5]), which operates with diode parameters of 700 keV, current up to 10 kA, and flattop pulse length up to 1 μs. This primary beam may be modulated using the proven techniques by Friedman et al. [2]. Note that the average acceleration gradient of 45 kV/cm and the peak acceleration gradient of about 80 kV/cm implied by Fig. 4 are well within the rf breakdown limit. If we assume an acceleration efficiency of 25 per cent, a secondary beam of more than 8 amps of current may be accelerated to 5 MeV in less than a meter in this proof-of-principle experiment.
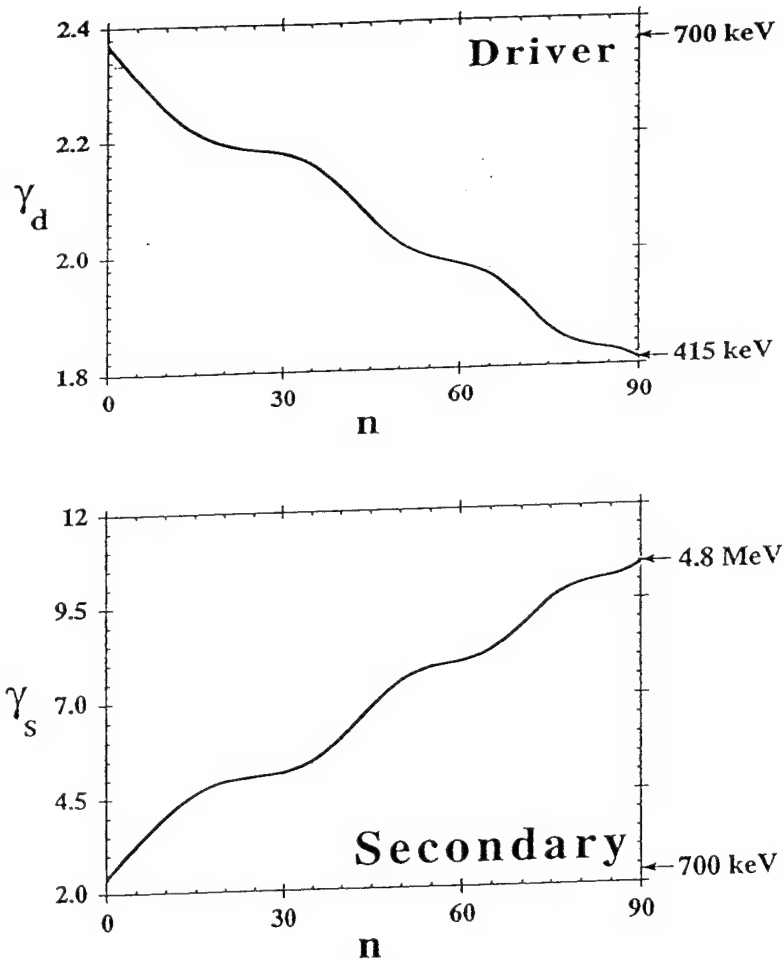

Figure 4. Evolution of the relativistic mass factors when the driver beam radius r_0 is modulated to compensate phase slippage: (a) the driver beam, (b) the secondary beam.

ISSUES

We shall address some of the issues which may affect the eventual usefulness of the twobetron. They concern the scaling laws, beam breakup instabilities, wakefield effects, effects of finite beam thickness, coupling among cavities, modification of rf characteristic by the intense driver beam, and the integrity of the primary beam modulation in the accelerating structure.

Scaling

The average energy gain per cavity by the secondary beam in the twobetron is

$$< E_s >= (16.3 \text{keV}) \times Q \times (I_d / 1 \text{kA}) \times (\Delta / a). \tag{8}$$

The transformer ratio, R, which is the ratio of the energy gain in the secondary beam to the energy loss in the primary beam, is

$$R = 0.803(a / \Delta). \tag{9}$$

The maximum amount of secondary beam current, I_s, that can be accelerated is limited to

$$I_s < \frac{I_d}{2R}. \tag{10}$$

Given a driver beam current, we cannot make the acceleration gradient (i.e., $<E_s>$) excessively high by using a very high Q cavity. A practical limit on $<E_s>$ is set by rf breakdown in the cavities [6].

In general, a transformer ratio R of the order of 10 seems achievable. A two-stage twobetron, in which the accelerated beam of the first stage is used as the driver beam in the second stage, will provide voltage multiplication by a factor of 100, while the output current is correspondingly much reduced [cf. Eq. 10].

Primary Beam Instabilties

The intense driver beam passing through a sequence of cavities is highly vulnerable to beam breakup instabilities (BBU [7-10]). However, we have recently found that BBU in an annular beam may be far less serious than a pencil beam [8]. Specifically, in the absence of other stabilizing mechanisms such as stagger tune and betatron frequency spread, the number of e-folds, (N, in BBU amplitude growth) over an accelerator of length z is given by [9]

$$N = \left(\frac{\omega_b z}{\beta_d c}\right)\left(\frac{\omega_b}{\omega_\beta}\right)\varepsilon Q_b, \tag{11}$$

where ω_b is the frequency of the deflecting mode with quality factor Q_b, ω_β is the betatron frequency associated with the focusing field, $\varepsilon = 0.0041(\beta_d/\gamma_d)(I_d/1kA)$ is the dimensionless coupling constant, and β_d, γ_d are defined in Eq. 5. For a solenoidal magnetic field of 10 kG and a dipole mode Q_b of 100, $N = 1.8$ for a 500 ns, 0.5 kA driver beam in a 90 cm accelerator structure, as in the numerical example.

We conjecture that the longitudinal (Robinson-like) instability [10] probably is not important for the twobetron, at least in the proposed proof-of-principle experiment. Unlike a circular accelerator, the present scheme is single-pass. Its acceleration length is quite short, its length is only slightly over one wavelength in the radius modulation. Moreover, the drive frequency may be adjusted to be on the "right side" of the structure frequency to avoid the Robinson-like instability.

In a preliminary particle simulation, we find that the current modulation is preserved on the primary beam, after it is made to propagate through the accelerating structure, using the beam and structure parameters that are being planned for a proof-of-principle experiment.

Wakefield Effects

We have also examined the effects of the transverse wake on the driver beam, and found that a nominal value of solenoidal field $B_0 = 10$ kG would render the effects of the transverse wakefield on the driver beam unimportant. Specifically, under the condition $\Omega \gg \omega/\gamma_d(1+\beta_d)$,where Ω is the nonrelativistic cyclotron frequency associated with B_0 and the other symbols are the same as in Eq. (5), the electron motion is adiabatic along the composite (DC + rf) magnetic field line. The maximum angular displacement, from the mean, is estimated to be

$$\ell_\theta = 0.52(c/\omega)(E_a/cB_o)\beta_d/(1-\beta_d) \tag{12}$$

where E_a is the maximum accelerating electric field experienced by the secondary beam. The maximum radial displacement is

$$\ell_r = \ell_\theta \lambda_L / \lambda_m, \tag{13}$$

where $\lambda_L = 2\pi\beta_d\gamma_d c/\Omega$ and λ_m is the axial wavelength associated with the modulation in the driver beam radius. For the parameters used in the numerical example, $\ell_\theta \leq 0.2$cm, and $\ell_r \leq 0.0058$cm. The spread in momentum, dp, in the

driver beam may introduce a variation in its annular beam radius, dr_o. It is estimated that

$$dr_o \leq [2(\lambda_L^2 / \lambda_m^2)\Delta + 0.083\lambda_L E_a / cB_o]dp / p \; , \tag{14}$$

where Δ is the amplitude of the modulation in the driver beam radius. Using the parameters in the numerical example [Fig. 4], we find $dr_o < 0.0061$ cm if $dp/p < 1$. Thus, the effectiveness of radius modulation is not affected by momentum spread.

RF Coupling Between Cavities

We have for simplicity assumed that the cavities are isolated from one another electromagnetically when the beam is absent. There are several ways to reduce the coupling among neighboring cavities. The inductive coupling at the annular slots, through which the driver beam passes, may be cancelled by the capacitive coupling at the center hole, and if necessary, by introducing additional holes near the rf electric field maximum (so as to increase the capacitive coupling) that is close to the outer wall of the cavity [Fig. 1]. Alternatively, conducting wires may be inserted radially across the annular gap to reduce the inductive coupling. Multiple pencil beams may also be used as the driver. These pencil beams pass through holes that are distributed annularly. In the event that the neighboring cavities are not completely isolated electromagnetically, a traveling wave formulation would be required; but the radius modulation that is proposed in this paper still provides an external control to ensure phase focusing.

The presence of intense space charge in the driver beam complicates matters substantially, as it is known to modify the rf characteristics in an unpredictable manner. Such modifications include a detune of the structure frequency and modification of the gap transit-time factor, especially if a virtual cathode is on the verge of being formed [2, 11]. Other modes may be excited. Indeed, mode competition is a major area that requires considerable attention in the twobetron concept.

Effect of Finite Thickness in the Driver Beam

The effect of finite thickness, τ, in the driver beam is found to be much less important than its mean radius, r_o. The finite beam thickness modifies Eq. 3 to read

$$\delta \approx -1.249(r_o - a) / a - 0.05(\tau / a)^2 . \tag{15}$$

58

The last term in Eq. 15 is usually much smaller than the first term even if τ and the radius modulation amplitude, Δ, are of the same order of magnitude (Eq. 6).

CONCLUDING REMARKS

In summary, the twobetron has the potential of converting many existing pulse power systems into compact rf accelerators that are suitable for industrial and medical applications. The driver beam is a modulated electron beam of annular shape and low energy. The secondary beam is an on-axis pencil beam. The secondary beam may reach an energy up to 10 MeV in one to two meters. Transformer ratio on the order of ten is considered feasible for each stage. Phase focusing and energy tunability of the accelerated beam may be provided by an external magnetic field, which controls the radius of the primary beam.

Excitation of the undesirable modes by the driver beam is perhaps the single most important issue in the twobetron concept.

ACKNOWLEDGMENTS

REFERENCES

1. G. Voss and T. Weiland, DESY Reports #M82-10 (1982) and M82-079 (1982); A. M. Sessler and S. S. Yu, Phys. Rev. Lett. **58**, 2439 (1987); M. A. Allen et al., *ibid.*, **63**, 2472 (1989); W. Gai et al., *ibid.*, **61**, 2765 (1988); H. Figueroa et al., *ibid.*, **60**, 2144 (1990); J. B. Rosenzweig et al., Phys. Fluids **B2**, 1376 (1990); A. M. Sessler et al., Part. Accel. **31**, 1277 (1990), Nuclear Instrum Meth. **A306**, 592 (1991); D. B. Hopkins et al., *ibid.*, **228**, 15 (1984); D. H. Whittum et al., Phys. Rev. **A43**, 294 (1991); Also, in AIP Conf. Proc. no. 279, Ed. J. Wurtele (1993).

2. M. Friedman and V. Serlin, Phys. Rev. Lett. **55**, 2860 (1985); M. Friedman et al., J. Appl. Phys. **64**, 3353 (1988); J. Krall and Y. Y. Lau, Appl. Phys. Lett. **52**, 431 (1988); Y. Y. Lau et al., IEEE Trans. Plasma Sciences **PS-18**, 553 (1990).

3. M. Friedman et al., Phys. Rev. Lett. **63**, 2468 (1989); Rev. Sci. Instrum. **61**, 171 (1990); Also, see Proceedings of SPIE Meetings, no. 1407 (1991), no. 1629 (1992), no. 1872 (1993); Ed. H. E. Brandt.

4. Ya. S. Derbenev, Y. Y. Lau, and R. M. Gilgenbach, Phys. Rev. Lett. **72**, 3025 (1994).

5. R. M. Gilgenbach et al., in Digest of Fifth IEEE Pulse Power Conference (IEEE, New York, 1985), p. 126.

6. G. A. Loew and J. W. Wang, SLAC Publication No. 4647 (May, 1988).

7. W. K. H. Panofsky and M. Bander, Rev. Sci. Instrum. **39**, 206 (1968). A recent experimental study of beam breakup in high current beams is reported by P. R. Menge et al., J. Appl. Phys. **75**, 1258 (1994).

8. Y. Y. Lau and J. W. Luginsland, J. Appl. Phys. **74**, 5877 (1993). In the line above Eq. (7) of this paper, the factor (I/1 kA) should read (I/17 kA).

9. V. K. Neil, L. S. Hall, and R. K. Cooper, Part. Accel. **9**, 213 (1979); P. B. Wilson, AIP Conf. Proc. No. 87, p. 452 (1982).

10. A. W. Chao, *Physics of Collective Beam Instabilities in High Energy Accelerators*, (Wiley, New York, 1993).

11. D. G. Colombant and Y. Y. Lau, Phys. Rev. Lett. **64**, 2320 (1990); Phys. Rev. **A45**, R2179 (1992).

Beam breakup instability in an annular electron beam

Y. Y. Lau and John W. Luginsland
Intense Energy Beam Interaction Laboratory and Department of Nuclear Engineering,
University of Michigan, Ann Arbor, Michigan 48109-2104

It is shown that an annular electron beam may carry six times as much current as a pencil beam for the same beam breakup (BBU) growth. This finding suggests that the rf magnetic field of the breakup mode is far more important than the rf electric field in the excitation of BBU. A proof-of-principle experiment is suggested, and the implications explored.

Annular electron beams have the capability of carrying a much higher current than a pencil beam. Besides the obvious fact that annular beams have a larger cross-sectional area, their limiting currents are significantly higher than those of a pencil beam when placed in a metallic drift tube. For this and other reasons, annular beams have recently been chosen as the preferred geometry to generate coherent, ultrahigh power microwaves.[1,2] They have also been used as the primary beam in several "two-beam accelerator" configurations.[3,4] These annular beams either encounter a sequence of modulating gaps, or simply glaze by a slow wave structure to generate a wake field in the case of two-beam accelerators.[3] The beam radius, the pill box radius, and the slow wave structure radius may all be of the same order of magnitude. The high current would then lead to the beam breakup instability (BBU)[5–8] and this concern motivates the present study.

BBU is usually analyzed for a pencil beam propagating along the center axis of a sequence of accelerating cavities. Many BBU calculations of practical interest assume that the accelerating unit is the familiar cylindrical pillbox cavity and that the dominant deflecting mode is the TM_{110} mode.[5,6,10] Extension to an annular beam is straightforward. Nevertheless, this calculation leads to several unexpected results and provides some new insights into BBU, to be reported in this communication.

It is well known that BBU is excited by the combined action of the rf magnetic field ($\mathbf{B}_1$) and the rf electric field ($\mathbf{E}_1$) of the deflecting modes:[5] $\mathbf{B}_1$ causes beam deflection through the Lorentz force and $\mathbf{E}_1$ causes mode amplification through the work done on the mode by the beam current $\mathbf{J}$. Our calculation strongly suggests that $\mathbf{B}_1$ is much more critical than $\mathbf{E}_1$ in contributing to BBU growth. Thus, an annular beam strategically placed near the minimum of the rf magnetic field would suffer far less beam breakup growth than a pencil beam that is centered on the cavity axis, where the magnetic field is large and the axial electric field is small. By the same argument, placing the annular beam very close to the wall of a metallic drift tube, at which the axial electric field is vanishingly small, cannot eliminate BBU growth because of the substantial deflecting magnetic field generated by the wall current. Toward the end of this communication, we propose an experiment which would unambiguously test the relative importance between the rf magnetic field and the rf axial electric field, as discussed here.

Consider an infinitesimally thin annular beam of radius r_0 inside a cylindrical pillbox of radius b. The beam carries a total current I and coasts at velocity v_0 with the corresponding relativistic factors γ and β. The drift tube is loaded with a slow wave structure, modeled by a series of cylindrical pillbox cavities, each of which supports the nonaxisymmetric TM_{110} mode.[3,5,6,10] The interaction between this mode and the beam causes BBU to be excited. In the limit $r_0 \to 0$, this is the basic model of BBU for a pencil beam. Since we are comparing the strength of BBU interaction for different values of r_0, we pretend that magnetic focusing is absent and that the quality factor Q of the deflecting mode is infinite.

Let $\mathbf{A}_1 = \hat{z} q(t)(\cos\theta)E(r)$ be the vector potential of the deflecting dipole mode in a cavity. For the fundamental TM_{110} mode, $E(r) = J_1(pr)$ represents the radial dependence of the axial electric field with J_1 being the Bessel function of order one and $p = 3.832/b$. The corresponding magnetic field is $\mathbf{B}_1 = \nabla \times \mathbf{A}_1$. The action of this mode on the beam is calculated as follows.

We divide the annular beam into N azimuthal segments (N large). The ith segment is located at $r = r_0$, $\theta = \theta_i = 2\pi i/N$, in the unperturbed state but is displaced radially by ξ_i and azimuthally by η_i when the deflecting mode is present. The linearized force law yields

$$-\gamma(\omega - kv_0)^2 \xi_i = (e/m_0)(v_0/c)qE'(r_0)\cos\theta_i, \qquad (1)$$

$$-\gamma(\omega - kv_0)^2 \eta_i = -(e/m_0)$$
$$\times (v_0/c)q[E(r_0)/r_0]\sin\theta_i, \qquad (2)$$

where the right-hand sides represent the components of the Lorentz force that causes beam deflection. In writing Eqs. (1) and (2), we have assumed a wave-like solution $\exp[j(\omega t - kz)]$ for the disturbances, with $j^2 = -1$, and we have used a prime to denote derivative with respect to the argument.

The instantaneous current J on the ith current filament is

$$\mathbf{J}_i(r,t) = \hat{z}\frac{I}{N}\frac{1}{r}\delta(r - r_0 - \xi_i)\delta\left(\theta - \theta_i - \frac{\eta_i}{r_0}\right), \qquad (3)$$

where δ is the Dirac delta function. The work done by this current filament on the deflecting mode is proportional to

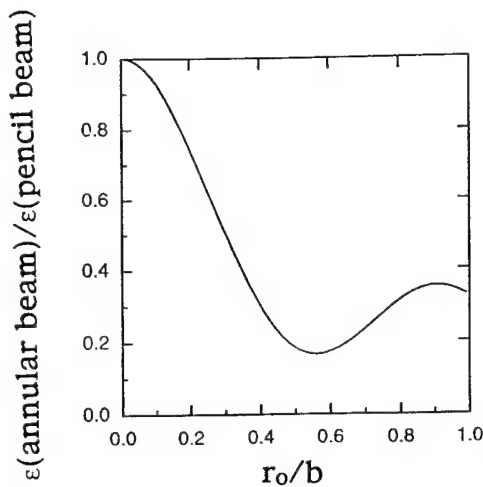$$W_i = \int dV\, \mathbf{A}_1 \cdot \mathbf{J}_i, \qquad (4)$$

FIG. 1. Comparison of the BBU coupling constant ϵ between an annular beam of radius r_0 and an on-axis pencil beam ($r_0 \to 0$) with the same total current.

where the volume integral is performed over the cavity. In evaluating W_i, we should retain only the rf component of $\mathbf{J}_i$ in Eq. (3), since only the rf current performs work on the breakup mode. Upon substituting Eqs. (1)–(3) into Eq. (4), and summing over all i, we find the total work done

$$W = \sum_{i=1}^{N} W_i = -\frac{LIe}{m_0} \frac{v_0}{c} q \frac{[E'(r_0)]^2 + [E(r_0)/r_0]^2}{\gamma (\omega - k v_0)^2} \qquad (5)$$

apart from a multiplicative constant that is independent of the beam's equilibrium position r_0. This energy transfer leads to growth of the BBU mode, which is described by the BBU dispersion relation:[8]

$$(\omega^2 - \omega_0^2)(\omega - k v_0)^2 = -2\omega_0^4 \epsilon = -2\omega_0^4 \epsilon_0 (\epsilon / \epsilon_0), \qquad (6)$$

where ϵ is the coupling constant and ω_0 is the breakup mode frequency. In writing the last form of Eq. (6), we normalize ϵ in terms of ϵ_0, the coupling constant for an on-axis, pencil beam ($r_0 \to 0$). For the TM_{110} mode, $E = J_1(pr)$ and $\epsilon_0 = 0.422 (\beta/\gamma)(I/1 \text{ kA})$. It is clear from Eq. (5) that

$$\frac{\epsilon}{\epsilon_0} = 2 \left\{ [J_1'(pr_0)]^2 + \left[\frac{J_1(pr_0)}{pr_0} \right]^2 \right\}, \qquad (7)$$

which compares the BBU strength between an annular beam and a pencil beam of the same current. Note that this ratio reduces to unity in the limit $r_0 \to 0$.

Equation (7) is plotted in Fig. 1 as a function of r_0/b. It is seen from this figure that ϵ/ϵ_0 may be as small as 0.17 when the annular beam is located at $r_0 = 0.56b$. Note also that this location coincides with the minimum of the rf magnetic field of the deflecting mode. What this means is that an annular beam placed at this location can carry as much as $1/0.17 = 6$ times the current as an on-axis pencil beam, and suffer the same BBU growth. Another point worth noting is that BBU growth retains significant strength even if the annular beam is very close to the wall of the drift tube (cf. $r_0 \to b$ in Fig. 1). This result is unex-

pected since $E_1 \to 0$ near a metallic wall. As a result, $\mathbf{J}_1 \cdot \mathbf{E}_1 \to 0$ and, superficially, one could hardly expect any transfer of power from the beam to drive the breakup mode.[9] The finite BBU strength as $r_0 \to b$ is another strong indication that the deflecting magnetic field is far more important than the axial rf electric field in driving BBU.

The importance of the rf magnetic field can be tested in an experiment in which a pencil beam is focused by a solenoidal magnetic field and is made to pass through a sequence of pillbox cavities, in which the first cavity is primed with microwaves at the TM_{110} mode.[10] BBU growth is monitored at the last cavity, before the beam exit. The above theory then predicts the *unusual* feature that BBU growth should be *much less* if the pencil beam is placed *off-axis*, than if the pencil beam were on-axis.[11] The BBU growth should be minimum if this pencil beam is placed at a distance of about 0.56 of the pillbox radius, where the rf magnetic field is minimum.

We also repeated the calculations for the higher order radial modes: TM_{120}, TM_{130}, TM_{140}, and TM_{150}. Fixing $r_0/b = 0.56$, the ratio ϵ/ϵ_0 equals 0.16, 0.012, 0.037, and 0.013 for these four higher order modes, respectively. Thus, the annular beam still suffers substantially lower BBU growth, in the higher order deflecting modes, than an on-axis pencil beam of the same current.

In conclusion, the rf magnetic field is found to be much more important than the rf electric field in contributing to BBU growth. A simple proof-of-principle experiment is proposed to test this new finding. Annular beams are far more stable than an on-axis pencil beam, as a result.

[1] V. Serlin and M. Friedman, Appl. Phys. Lett. **62**, 2772 (1993); Y. Y. Lau, M. Friedman, J. Krall, and V. Serlin, IEEE Trans. **PS-18**, 553 (1990) and references therein; M. Friedman, Y. Y. Lau, J. Krall, and V. Serlin, U. S. Patent 5,132,638 (issued July 21, 1992); J. Krall, M. Friedman, Y. Y. Lau, and V. Serlin, IEEE Trans. **EMC-34**, 22 (1992).
[2] C. Chen, P. Catraras, and G. Bekefi, Appl. Phys. Lett. **62**, 1579 (1993); See also, "Intense Microwave and Particle Beams III," Proc. Soc. Photo Opt. Instrum. Eng. SPIE **1629** (1992).
[3] G. Voss and T. Weiland, "The wakefield acceleration mechanism," Deutsches Electron-Synchrotron Internal Report DESY #M82-10 (1982); M82-079 (1982), Hamburg, Germany.
[4] M. Friedman, J. Krall, Y. Y. Lau, and V. Serlin, Phys. Rev. Lett. **63**, 2468 (1989).
[5] W. K. H. Panofsky and M. Bander, Rev. Sci. Instrum. **39**, 206 (1968); R. H. Helm and G. A. Loew, in *Linear Accelerators*, edited by R. P. Lapostolle and A. L. Septier (North-Holland, Amsterdam, 1970), p. 173.
[6] V. K. Neil, L. S. Hall, and R. K. Cooper, Part. Accel. **1**, 111 (1970); **9**, 213 (1979).
[7] A. W. Chao, B. Richter, and C. Y. Yao, Nucl. Instrum. Methods **178**, 1 (1980); K. A. Thompson and R. D. Ruth, Phys. Rev. D **41**, 964 (1990); R. L. Gluckstern, F. Neri, and R. K. Cooper , Part. Accel. **23**, 37 (1988); C. L. Bohn and J. R. Delayen, Phys. Rev. A **45**, 5964 (1992); D. Chernin and A. Mondeli, Part. Accel. **24**, 685 (1985); G. Decker and J. M. Wang, Phys. Rev. D **38**, 980 (1988); W. E. Martin, G. J. Caporaso, W. M. Fawley, D. Prosnitz, and A. G. Cole, Phys. Rev. Lett. **54**, 685 (1985); D. Colombant, Y. Y. Lau, and D. Chernin, Part. Accel. **35**, 193 (1991).
[8] Y. Y. Lau, Phys. Rev. Lett. **63**, 1141 (1989).

[9]The rate of power transfer is proportional to the gradient of E_1, rather than E_1 itself. This may be seen when one substitutes Eq. (3) into Eq. (4) and performs integration by parts.

[10]P. R. Menge, R. M. Gilgenbach, and Y. Y. Lau, Phys. Rev. Lett. **69**, 2372 (1992); P. R. Menge, R. M. Gilgenbach, and R. Bosch, Appl. Phys. Lett. **61**, 642 (1992).

[11]BBU growth on a pencil beam that is placed off-center can be easily calculated by using Eq. (4) instead of Eq. (5). We pretend that the total beam current is carried by the ith filament that enters Eq. (4). Although the BBU growth of such an off-center beam depends on θ_i, its coupling constant ϵ is still much less than ϵ_0, the value for an on-axis beam.

63

A Model of Injection Locked Relativistic Klystron Oscillator*

J.W. Luginsland, Y.Y. Lau, K. Hendricks[1], and P. D. Coleman[2]

Intense Energy Interaction Laboratory

Department of Nuclear Engineering

The University of Michigan

Ann Arbor, MI 48109-2104

Abstract

By the use of a simple model, we explicitly incorporate the coupling between the driver cavity and the booster cavity in a relativistic klystron amplifier (RKA). We show that this RKA configuration may turn into an injection locked oscillator only when the beam current is sufficiently high. Other features revealed by this model include: the downshifted frequency mode ("0" mode) is unstable whereas the upshifted frequency mode ("π" mode) is stable; the growth rate of the "0" mode is relatively mild so that the oscillation can start only in an injection locked mode; the oscillation does not require the presence of reflected electrons; and the separation of the cavities must be sufficiently short. These, and other features, are found to be in qualitative agreement with the recent experiments on the injection locked relativistic klystron oscillator (RKO) that were conducted at the Phillips Laboratory.

1

I. Introduction

Current modulation of an intense relativistic electron beam (IREB) remains a challenging and active research problem [1] with applications to high power microwave (HPM) production [2-4], and to some accelerator schemes that use an IREB as a driver [5,6]. Recently, a series of experiments were performed at Phillips Laboratory [7], where an IREB was placed in a relativistic klystron amplifier (RKA) geometry [2-4], with the driver and booster cavities sufficiently close to couple to one another. This cavity coupling caused the structure to oscillate at a frequency different from the driver frequency. This oscillation persisted after the external drive was shut off, but its appearance has always required an input drive and a sufficiently large DC current. Thus, the device operated as an injection-locked relativistic klystron oscillator (RKO). It provided 40% to 60% of current modulation on the DC beam when the gap separation is on the order of only 10 cm, as opposed to 30 cm in a typical RKA geometry with similar frequency (at 1.3 GHz), beam current and drift tube diameter. Another interesting feature is that virtual cathodes did not seem to have been formed for the operation of this RKO. The feedback, therefore, was due only to the electromagnetic coupling among the two cavities, and not to the reflected electrons as in previous works [8].

In this paper, we present a simple analytic model, explicitly including the effect of cavity coupling. The results of this model demonstrate several features that were observed in the RKO experiments mentioned above. They are summarized in the abstract and are discussed further below.

2

II.   Model

Consider an annular intense relativistic electron beam (IREB) with radius r_b propagating in a drift tube of radius r_w and passing by two cavities [Fig. 1]. The first cavity, with gap voltage A(t), is driven by an external source. The second cavity, with gap voltage B(t) and located at a distance d downstream, is driven by the beam. When d is sufficiently small, there would be coupling between A and B even if the drift tube is cutoff to the frequency of operation. In the absence of the beam, the steady state voltages A and B are either in phase ("0" mode) or 180° out of phase ("pi" mode). That is, there is no phase delay between the two cavities, when the beam is absent, because the drift tube is cutoff [9].

To study this effect, we start by writing down the circuit equations of the two cavities, each having a natural frequency ω_o, and quality factor Q. The evolution of the gap voltages A and B is governed by

$$\left[\frac{d^2}{dt^2}+\frac{\omega_o}{Q}\frac{d}{dt}+\omega_o^2\right]A(t)=\omega_o^2 CB(t) \ , \tag{1}$$

$$\left[\frac{d^2}{dt^2}+\frac{\omega_o}{Q}\frac{d}{dt}+\omega_o^2\right]B(t)=-j\omega_o^2 ZI+\omega_o^2 CA(t) \ , \tag{2}$$

where C (<< 1) is the dimensionless, real constant measuring the degree of coupling between the two gaps when the beam is absent [9], and Z is defined such that ZQ is the impedance (in Ohms) at the second gap. Equation (1) expresses the excitation of the gap voltage A by the gap voltage B as a result of cavity coupling C. Since we are concentrating on the RKO operation, we ignore the external rf drive on the gap voltage A, and we envision the effect of this external drive to enter only as the initial condition on A, at the instant when the external drive is shut off. Equation (2)

3

66

describes the excitation of the second gap by the rf current, I, and by the first gap voltage A because of the cavity coupling.

As in the usual klystron theory, the rf current I at the second gap is due to the voltage at the first gap. In the case of an IREB of DC current I_o, it is given by [1]

$$I = j\left(\frac{A}{R}\right)\sin(k_p d)e^{-j\theta} \ . \tag{3}$$

In Eq. (3), R is the rf beam impedance (in Ohms), $\theta = \omega d/\beta c$ is the phase delay of the beam mode, and

$$k_p d = \frac{\sqrt{\alpha}}{\beta^2 \gamma}\left(\frac{\omega d}{c}\right) \ , \qquad R = \frac{511 kV}{I_o}\gamma^2\beta\sqrt{\alpha} \ , \tag{4}$$

$$\alpha = \frac{I_o}{I_s \beta \gamma^3} \qquad , \qquad I_s = 8.5 kA / \ell n(r_w / r_b) \ ,$$

where β and γ are the usual relativistic mass factors associated with the DC beam, and c is the speed of light. Upon inserting Eq. (3) into Eq. (2), we obtain two equations (1), (2) in two unknowns A, B. Assuming $\exp(j\omega t)$ dependence for both A and B, we obtain the dispersion relation for ω which may easily be solved to yield

$$\omega = \omega_o\left[1 + \frac{j}{2Q} \pm \frac{C}{2}\sqrt{1 + \frac{Z}{CR}\sin(k_p d)e^{-j\theta}}\right] \ . \tag{5}$$

Equation (5) gives the temporal growth rate of the coupled-cavity RKO in terms of the circuit parameters (ω_o, Q, C, d, Z) and the beam parameters (R, k_p, θ). In the next section, we present

4

67

the numerical results using parameters similar to those in the experiments [7]. We shall also describe the interesting features revealed by the dispersion relation (5).

III.   Numerical Results

We shall first establish the numerical values of the parameters from the experiments [7]. In the cold tests, it was observed that when the two cavities are coupled, there was a frequency shift of ± 7 MHz from the natural frequency of 1.27 GHz that was measured for an isolated cavity. Thus, when the beam is absent, $R \rightarrow \infty$ from Eq. (4) and we obtain from Eq. (5) the cold tube coupled-cavity natural frequencies

$$\omega = \omega_o \left[1 + \frac{j}{2Q} \pm \frac{C}{2} \right] , \tag{6}$$

with $\omega_o = 2\pi \times 1.27$ GHz and $\omega_o C/2 = 2\pi \times 7$ MHz. This yields the coupling constant $C = 0.0112$. In Eq. (6), the (+) sign corresponds to the "π" mode and the (-) sign corresponds to the "0" mode. Substitution of Eq. (6) into Eq. (1), in which d/dt is replaced by $j\omega$, shows that the gap voltages A and B are 180° out of phase for the "π" mode, and that they are in phase for the "0" mode.

The value of Q to be used is uncertain. There is the cold tube value, in excess of 400 according to measurements [7], and there is the substantially reduced value of the beam-loaded Q, which depends on the beam current. Let us arbitrarily set the beam-loaded Q to be 100, say. The value of Z may be estimated from Eq. (2) which shows that, in the absence of cavity coupling [i.e., C = 0], the magnitude of the gap voltage B equals to QZ times the magnitude of the rf current I there. From this definition of Z, we estimate that $Z = 1.6 \, \Omega$ when Q is assigned to be 100. The

5

68

beam parameters R, k_p, and θ, are determined as follows. We set the beam voltage at 400 keV, beam current $I_o = 12$ kA, with mean beam radius $r_b = 6.85$ cm in a drift tube of radius $r_w = 7.65$ cm. Using these parameters, we find $\gamma = 1.783$, $\beta = 0.828$, $I_s = 77$ kA, $\alpha = 0.033$, $k_p = 0.0398$ cm^{-1} and R = 20.4 Ω. If we set the gap separation at d = 11 cm, then $k_p d = 0.437$ and $\theta = 3.55$. Using these parameters in Eq. (5), we find

$$\omega = \omega_0(1.0023 + 0.0127j) \qquad \text{"}\pi\text{" mode} \qquad (7a)$$
$$\omega = \omega_0(0.9976 - 0.00266j) \qquad \text{"0" mode} \qquad (7b)$$

Equations (7a) and (7b) show the following.

A. The "π" mode is stable and the "0" mode is unstable.

B. For the "0" mode, there is a downshift in frequency from $f_o = \omega_o/2\pi = 1.27$ GHz, by the amount of 1.27 GHz x (1 - 0.9976) = 3.05 MHz. That is, the mode is upshifted from the cold-tube "0" mode frequency by the amount of 7 MHz - 3.05 MHz = 3. 95 MHz, and this upshift is beam induced.

C. The growth of the "0" mode, according to Eq. (7b), is relatively mild. The total number of e-folds in a time $\tau = 100$ ns is $\omega_i\tau = 2.12$. This mild growth implies that, for an IREB whose pulselength is on the order of 100 ns, the manifestation of RKO behavior may require an external drive so that there is already a significant rf gap voltage by the time this external rf drive is shut off.

D. The "0" mode is unstable only if the DC beam current is sufficiently high. This is obvious since in the limit of zero current, the mode is damped [cf. Eq. (6)]. Using the parameters given in the paragraph preceeding Eq. (7a), we find that the threshold DC beam current for the onset of growth for the "0" mode is 7.2 kA. Similar levels of threshold current were observed in the experiments.

E. Upon inserting Eq. (7b) into Eq. (1), in which d/dt is replaced by $j\omega$, we find the ratio of the gap voltage to be $|B / A| = 1.43$ using the parameters in the paragraph preceeding Eq (7a). This number is in reasonable agreement with experimental observations.

Points A - E are features revealed by the experiments [7]. We wish to add the following points which also seem to corroborate the experimental results.

F. The instability does not require the formation of a virtual cathode. That is, there is no need to invoke reflected electrons to provide the feedback that is usually required for oscillation [8].

G. The cavity separation must be sufficiently short to provide appreciable coupling between the two cavities.

H. The operation of this injection-locked RKO is restricted only to a narrow range of gap separation, d, once the other circuit parameters, beam parameters, and the level of rf drive are fixed. There are three reasons for this: (i) The cavity coupling diminishes rapidly with increasing d, as the drift tube is below cutoff. (ii) If d is too small, there is little buildup in the current modulation from the driver cavity to the second one downstream. (iii) The ballistic phase θ that appears in Eq. (5) is proportional to d. Note that (i) is quantified in Eq. (5) through the coupling constant C and (ii) is quantified in Eq. (5) through the factor $\sin(k_p d)$.

IV.   Concluding Remarks

While we are able to construct a relatively simple model which appears to be capable of explaining many features observed in the recent injection-locked RKO experiments, it must be kept in mind that there are many uncertainties in the model. Chief among them are the values of Q and the coupling constant C. The beam-loaded Q depends on the current modulation, which depends

7

not only on the DC current, but also on the level of rf drive and the gap separation d. The value of C is a sensitive function of gap separation, and the one we use in this paper is inferred from the cold tube measurements. There is also uncertainty in the value of the gap impedence Z because the "gap transit time factor", which is significantly affected by the DC space charge effects associated with an IREB, will make the determination of Z far from a trivial matter [10]. Unfortunately, the *conceptually* simple mechanism proposed in this paper may not be easy to verify in particle-in-cell codes. The main reason is that the mild growth envisioned would require a long simulation time. To shorten the simulation time by raising the beam current runs into the possibility of triggering virtual cathode formation. In addition, there may be marked difference between the "numerical Q", the cold-tube Q, and the hot-tube Q in the experiments. As explained above, our model shows that the threshold current may depend sensitively both on Q and on the gap separation d.

In spite of the great uncertainties in several crucial parameters, we find it remarkable that a reasonable choice of parameters does yield reasonable agreement with observations, based just on the simple analytic model.

V.   Acknowledgements

VI.   Figure Caption

Fig. 1   The model

71

References

1. M. Friedman, and V. Serlin, Phys. Rev. Lett. **55**, 2860 (1985); M. Friedman, J. Krall, Y.Y. Lau, and V. Serlin, J. Appl. Phys. **64**, 3353 (1988); M. Friedman et al., Phys. Rev. Lett. **74**, 322 (1995).

2. See, e.g., J. Benford, and J. Swegle, *High Power Microwaves* (Artech House, Norwood, MA, 1992).

3. M. Friedman, J. Krall, Y.Y. Lau, and V. Serlin, Rev. Sci. Instrum. **61**, 171 (1990); Y. Y. Lau, J. Krall, M. Friedman, V. Serlin, IEEE Trans. Plasma Sci. **18**, 553 (1990); M. Friedman and V. Serlin, Proc. SPIE Vol. 1872, p. 2 (1993); M. Friedman et al., Phys. Rev. Lett. **75**, 1214 (1995).

4. G. Bekefi, P. Cateravas, C. Chen and I. Mastovsky, Proc. SPIE Vol. 1872, p. 25 (1993); M.V. Fazio et. al., IEEE Trans. **PS-22**, 740 (1994); J.S. Levine, and B.D. Hartenbeck, Appl. Phys. Lett. **65**, 2133 (1994).

5. M. Friedman, J. Krall, Y.Y. Lau, and V. Serlin, Phys. Rev. Lett. **63**, 2468 (1989).

6. Ya. S. Derbenev, Y.Y. Lau, and R.M. Gilgenbach, Phys. Rev. Lett. **72**, 3025 (1994).

7. K.J. Hendricks et. al., to be published (1995).

8. M. Friedman, V. Serlin, A. Drobot, and L. Seftor, J. Appl. Phys. **56**, 2459 (1984); M. Friedman, V. Serlin, A. Drobot, and A. Modelli, IEEE Trans. **PS-14**, 201 (1986); H. Uhm, IEEE Trans. **PS-22**, 5 (1994).

9. If an electromagnetic wave is allowed to travel between two cavities, there would then be a phase shift between the gap voltages. Models that include this phase delay may be found in D. G. Colombant and Y. Y. Lau, J. Appl. Phys. **72**, 3874 (1992). In the present paper, since the drift tube is cutoff to the electromagnetic waves, a sinusoidal steady state voltage on one gap does not induce a phase shift in the voltage on the other gap, when the beam is absent.

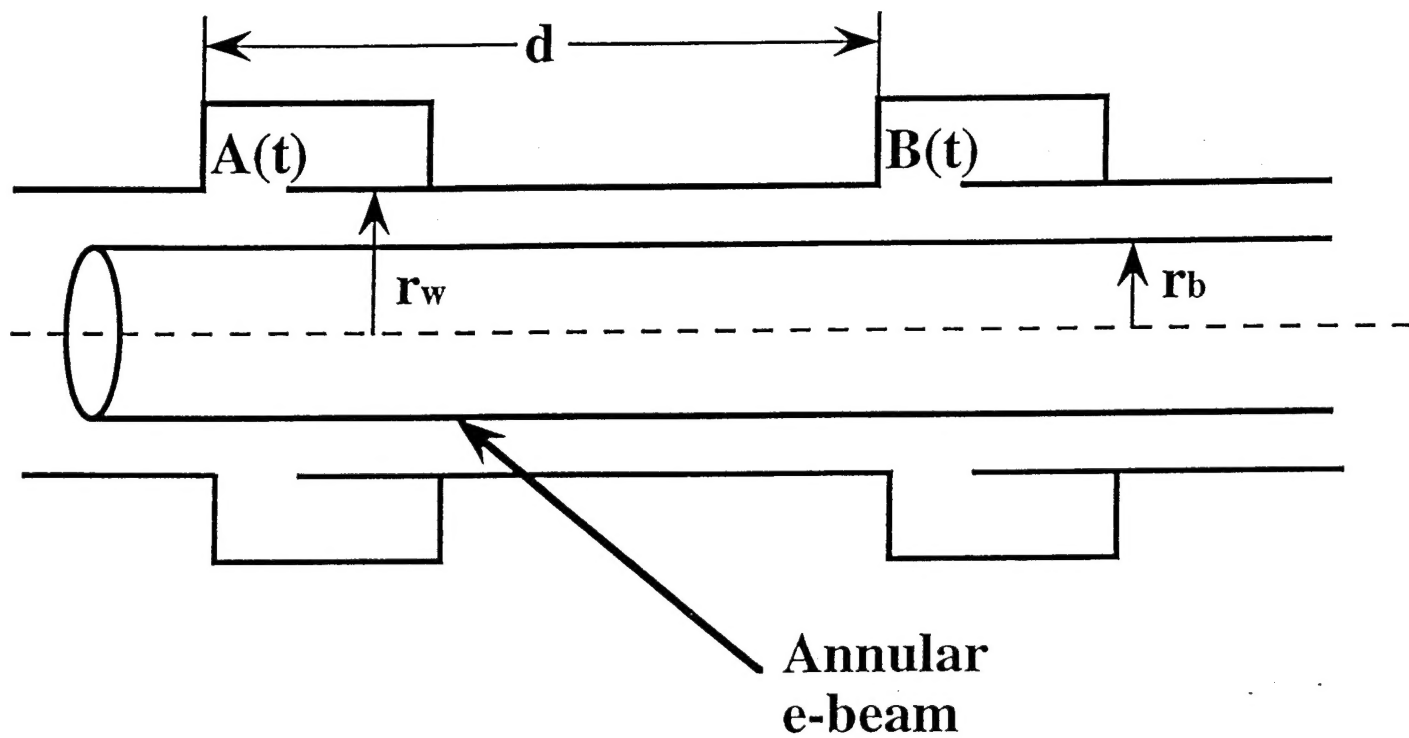10. D.G. Colombant, and Y.Y. Lau, Phys. Rev. Lett. **64**, 2320 (1990).

72

Fig. 1   The model